antibody directed against the hepatitis C virus E2 protein. J Virol 82:1047–1052.

Pestka JM, Zeisel MB, Bläser E, Schürmann P, Bartosch B, Cosset FL, Patel AH, Meisel H, Baumert J, Viazov S, Rispeter K, Blum HE, Roggendorf M, Baumert TF. 2007. Rapid induction of virus-neutralizing antibodies and viral clearance in a single-source outbreak of hepatitis C. Proc Natl Acad Sci USA 104:6025–6030.

Saito T, Watanabe H, Shao L, Okumoto K, Hattori E, Sanjo M, Misawa K, Suzuki A, Takeda T, Sugahara K, Ito JI, Saito K, Togashi H, Kawata S. 2004. Transmission of hepatitis C virus quasispecies between human adults. Hepatol Res 30:57–62.

Sasayama M, Deng L, Kim SR, Ide Y, Shoji I, Hotta H. 2010. Analysis of neutralizing antibodies against hepatitis C virus in patients who were treated with pegylated-interferon plus ribavirin. Kobe J Med Sci 56:E60–E66.

Scheel TK, Gottwein JM, Jensen TB, Prentoe JC, Hoegh AM, Alter HJ, Eugen-Olsen J, Bukh J. 2008. Development of JFH1-based cell culture systems for hepatitis C virus genotype 4a and evidence for cross-genotype neutralization. Proc Natl Acad Sci USA 105:997–1002.

Tarr AW, Owsianka AM, Timms JM, McClure CP, Brown RJ, Hickling TP, Pietschmann T, Bartenschlager R, Patel AH, Ball JK. 2006. Characterization of the hepatitis C virus E2 epitope defined by the broadly neutralizing monoclonal antibody AP33. Hepatology 43:592–601.

Wakita T, Pietschmann T, Kato T, Date T, Miyamoto M, Zhao Z, Murthy K, Habermann A, Kräusslich HG, Mizokami M, Bartenschlager R, Liang TJ. 2005. Production of infectious hepatitis C virus in tissue culture from a cloned viral genome. Nat Med 11:791–796.

Zhong J, Gastaminza P, Cheng G, Kapadia S, Kato T, Burton DR, Wieland SF, Uprichard SL, Wakita T, Chisari FV. 2005. Robust hepatitis C virus infection in vitro. Proc Natl Acad Sci USA 102:9294–9299.

frontiers in
MICROBIOLOGY

MINI REVIEW ARTICLE
published: 10 January 2012
doi: 10.3389/fmicb.2011.00278

Molecular mechanism of hepatitis C virus-induced glucose metabolic disorders

Ikuo Shoji*, Lin Deng and Hak Hotta

Division of Microbiology, Center for Infectious Diseases, Kobe University Graduate School of Medicine, Kobe, Japan

Edited by:
Yasuko Yokota, National Institute of Infectious Diseases, Japan

Reviewed by:
Koji Ishii, National Institute of Infectious Diseases, Japan
Kohji Moriishi, University of Yamanashi, Japan

****Correspondence:***
Ikuo Shoji, Division of Microbiology, Center for Infectious Diseases, Kobe University Graduate School of Medicine, 7-5-1 Kusunoki-cho, Chuo-ku, Kobe, Hyogo 650-0017, Japan.
e-mail: ishoji@med.kobe-u.ac.jp

Hepatitis C virus (HCV) infection causes not only intrahepatic diseases but also extrahepatic manifestations, including metabolic disorders. Chronic HCV infection is often associated with type 2 diabetes. However, the precise mechanism underlying this association is still unclear. Glucose is transported into hepatocytes via glucose transporter 2 (GLUT2). Hepatocytes play a crucial role in maintaining plasma glucose homeostasis via the gluconeogenic and glycolytic pathways. We have been investigating the molecular mechanism of HCV-related type 2 diabetes using HCV RNA replicon cells and HCV J6/JFH1 system. We found that HCV replication down-regulates cell surface expression of GLUT2 at the transcriptional level. We also found that HCV infection promotes hepatic gluconeogenesis in HCV J6/JFH1-infected Huh-7.5 cells. HCV infection transcriptionally up-regulated the genes for phosphoenolpyruvate carboxykinase (PEPCK) and glucose 6-phosphatase (G6Pase), the rate-limiting enzymes for hepatic gluconeogenesis. Gene expression of PEPCK and G6Pase was regulated by the transcription factor forkhead box O1 (FoxO1) in HCV-infected cells. Phosphorylation of FoxO1 at Ser319 was markedly diminished in HCV-infected cells, resulting in increased nuclear accumulation of FoxO1. HCV NS5A protein was directly linked with the FoxO1-dependent increased gluconeogenesis. This paper will discuss the current model of HCV-induced glucose metabolic disorders.

Keywords: HCV, diabetes, gluconeogenesis, GLUT2, FoxO1, JNK, NS5A

INTRODUCTION

Hepatitis C virus (HCV) is a positive-sense, single stranded RNA virus that belongs to the genus *Hepacivirus* of the family *Flaviviridae*. The approximately 9.6-kb HCV genome encodes a unique open reading frame that is translated into a polyprotein of about 3,000 amino acids, which is cleaved by cellular signalases and viral proteases to generate at least 10 viral proteins, such as core, envelope 1 (E1) and E2, p7, NS2, NS3, NS4A, NS4B, NS5A, and NS5B (Choo et al., 1991; Lemon et al., 2007).

Hepatitis C virus is the main cause of chronic hepatitis, liver cirrhosis, and hepatocellular carcinoma. More than 170 million people worldwide are chronically infected with HCV (Poynard et al., 2003). Persistent HCV infection causes not only liver diseases but also extrahepatic manifestations. It is well established that HCV perturbs the glucose metabolism, leading to insulin resistance and type 2 diabetes in predisposed individuals. Several epidemiological, clinical, and experimental data suggested that HCV infection serves as an additional risk factor for the development of diabetes (Mason et al., 1999; Negro and Alaei, 2009; Negro, 2011). HCV-related glucose metabolic changes and insulin resistance and diabetes have significant clinical consequences, such as accelerated fibrogenesis, increased incidence of hepatocellular carcinoma, and reduced virological response to interferon (IFN)-α-based therapy (Negro, 2011). Therefore, it is very important to clarify the molecular mechanism of HCV-related diabetes. However, the precise mechanisms are poorly understood.

Experimental data suggest a direct interference of HCV with the insulin signaling pathway. Transgenic mice expressing HCV core gene exhibit insulin resistance (Shintani et al., 2004; Koike, 2007). In this transgenic mice model, both tyrosine phosphorylation of the insulin receptor substrate (IRS)-1 and IRS-2 are decreased. These decreases are recovered when the proteasome activator PA28γ is deleted, suggesting that the HCV core protein suppresses insulin signaling through a PA28γ-dependent pathway (Miyamoto et al., 2007). Several other reports also showed a link of the HCV core protein with insulin resistance (Kawaguchi et al., 2004; Pazienza et al., 2007).

Hepatocytes play a crucial role in maintaining plasma glucose homeostasis by adjusting the balance between hepatic glucose production and utilization via the gluconeogenic and glycolytic pathways, respectively. Gluconeogenesis is mainly regulated at the transcriptional level of the glucose 6-phosphatase (G6Pase) and phosphoenolpyruvate carboxykinase (PEPCK) genes, whereas glycolysis is mainly regulated by glucokinase (GK). Gluconeogenesis and glycolysis are coordinated so that one pathway is highly active within a cell while the other is relatively inactive. It is well known that increased hepatic glucose production via gluconeogenesis is a major feature of type 2 diabetes (Clore et al., 2000).

To identify a novel mechanism of HCV-related diabetes, we have been investigating the effects of HCV on glucose production in hepatocytes using HCV RNA replicon cells (Lohmann et al., 1999) and HCV J6/JFH1 cell culture system (Lindenbach et al., 2005; Wakita et al., 2005; Bungyoku et al., 2009). We previously reported that HCV replication suppresses cellular glucose uptake through down-regulation of cell surface expression of glucose transporter 2 (GLUT2; Kasai et al., 2009). Furthermore, we

recently reported that HCV promotes hepatic gluconeogenesis via an NS5A-mediated, forkhead box O1 (FoxO1)-dependent pathway, resulting in increased cellular glucose production in hepatocytes (Deng et al., 2011). This paper discusses our current model for HCV-induced glucose metabolic disorders.

HCV REPLICATION DOWN-REGULATES CELL SURFACE EXPRESSION OF GLUT2

The uptake of glucose into cells is conducted by the facilitative glucose carrier, glucose transporters (GLUTs). GLUTs are integral membrane proteins that contain 12 membrane-spanning helices. To date, a total of 14 isoforms have been identified in the GLUT family (Wu and Freeze, 2002; Macheda et al., 2005; Godoy et al., 2006). Glucose is transported into hepatocytes by GLUT2. We previously reported that HCV J6/JFH1 infection suppresses hepatocytic glucose uptake through down-regulation of surface expression of GLUT2 in human hepatoma cell line, Huh-7.5 cells (Kasai et al., 2009). We also demonstrated that GLUT2 expression in hepatocytes of the liver tissues from HCV-infected patients was significantly lower than in those from patients without HCV infection. Our data suggest that HCV infection down-regulates GLUT2 expression at transcriptional level. We are currently analyzing transcriptional control of human GLUT2 promoter in HCV replicon cells as well as in HCV J6/JFH1-infected cells.

HCV INFECTION PROMOTES HEPATIC GLUCONEOGENESIS

Then we analyzed hepatic glucose production and expression of transcription factors using HCV replicon cells and HCVcc system in order to clarify a role of HCV infection in glucose metabolic changes. Hepatic glucose production is usually regulated by gluconeogenesis and glycolysis. Therefore, we examined whether HCV infection induces gluconeogenesis or glycolysis. We found that the PEPCK and G6Pase genes were transcriptionally up-regulated in J6/JFH1-infected cells (**Figure 1**). On the other hand, the GK gene was transcriptionally down-regulated in HCV-infected cells. We obtained similar data in HCV replicon cells (both in subgenomic replicon cells and full-genomic replicon cells). When HCV replication was suppressed by IFN treatment, the up-regulation of PEPCK and G6Pase gene expression as well as the down-regulation of GK gene expression were canceled. From these results, HCV infection selectively up-regulates PEPCK and G6Pase genes, whereas HCV infection down-regulates GK gene (Deng et al., 2011).

Both HCV replicon cells and HCV-infected cells produced greater amounts of glucose than the control cells. IFN treatment canceled the enhanced glucose production in HCV replicon cells as well as in HCV-infected cells. G6P is an important precursor molecule that is converted to glucose in the gluconeogenesis pathway (**Figure 1**). Our metabolite analysis showed that a significantly higher level of G6P was accumulated in HCV-infected cells than in the control cells, suggesting that HCV indeed promotes hepatic gluconeogenesis to cause hyperglycemia. There is a trend toward an increase in gluconeogenesis in HCV-infected cells (**Figure 1**).

HCV SUPPRESSES FoxO1 PHOSPHORYLATION AT Ser319, LEADING TO THE NUCLEAR ACCUMULATION OF FoxO1

It has been reported that G6Pase, PEPCK, and GK are regulated by certain transcription factors, including FoxO1 (Hirota et al., 2008), hepatic nuclear factor 4α (HNF-4α; Hirota et al.,

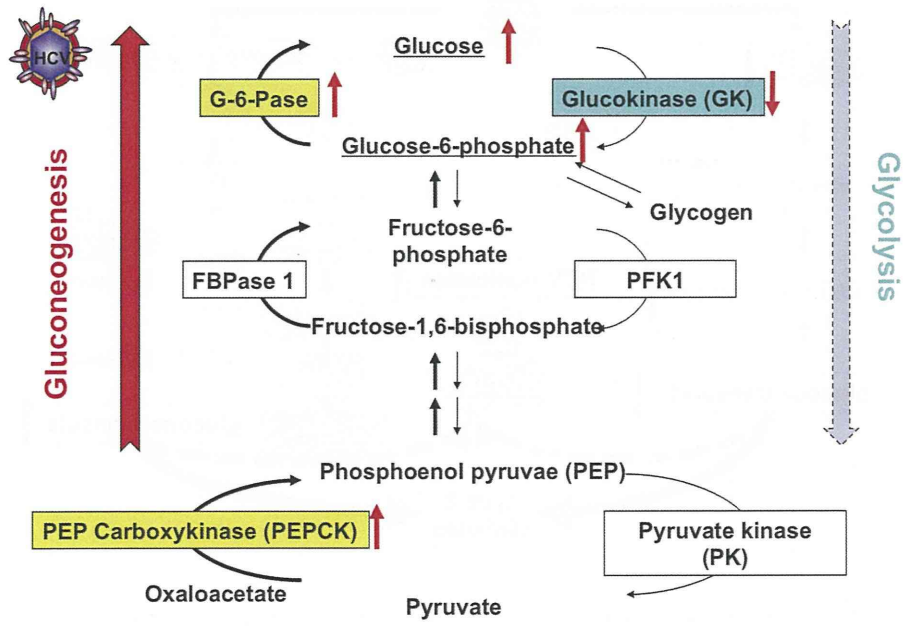

FIGURE 1 | Regulation of Gluconeogenesis and Glycolysis in the HCV-infected cells. HCV infection promotes gluconeogenesis via transcriptional up-regulation of the genes for PEPCK and G6Pase, the rate-limiting enzymes for hepatic gluconeogenesis, and transcriptional down-regulation of the gene for GK, the rate-limiting enzyme for hepatic glycolysis.

2008), Krüppel-like factor 15 (KLF15; Takashima et al., 2010), and cyclic AMP (cAMP) response element binding protein (CREB; Rozance et al., 2008). While we were analyzing these factors in both HCV replicon cells and HCV J6/JFH1-infected cells, we found the involvement of the FoxO1 in the transcriptional activation of G6Pase and PEPCK (Deng et al., 2011). It is known that the FoxO1 enhances gluconeogenesis through the transcriptional activation of various genes, including G6Pase and PEPCK (Gross et al., 2008). The function of FoxO1 is regulated by post-translational modifications, including phosphorylation, ubiquitylation, and acetylation (Tzivion et al., 2011). The phosphorylated form of FoxO1 is exported from the nucleus to the cytosol, resulting in loss of its transcriptional activity (**Figure 2**). Phosphorylation status of FoxO1 at Ser319 is critical for FoxO1 nuclear exclusion (Zhao et al., 2004). Although the total amounts of FoxO1 protein were unchanged, FoxO1 phosphorylation at Ser319 was markedly suppressed in HCV-infected cells compared to that in the mock-infected cells. It is known that the FoxO1 is phosphorylated by the protein kinase Akt and is exported from the nucleus to the cytosol, resulting in loss of its transcriptional activity (Tzivion et al., 2011). The majority of FoxO1 was accumulated in the nuclear fraction in HCV-infected cells, whereas in control cells FoxO1 was distributed in both the nuclear and cytoplasmic fractions. Akt phosphorylation was enhanced in HCV-infected cells, although the protein levels of total Akt protein were comparable, which is consistent with the report by Burdette et al. (2010). Our findings suggest an interesting scenario in which the HCV-mediated suppression in FoxO1 phosphorylation is caused by an unknown mechanism independent of Akt activity.

HCV-INDUCED JNK ACTIVATION IS INVOLVED IN THE SUPPRESSION OF FoxO1 PHOSPHORYLATION

It is known that the stress-sensitive serine/threonine kinase JNK regulates FoxO at multiple levels (van der Horst and Burgering, 2007; Karpac and Jasper, 2009). We demonstrated that HCV infection induces phosphorylation and activation of JNK in a time-dependent manner, which is similar to that observed for the suppression of FoxO1 phosphorylation. As a result, c-Jun, a key substrate for JNK, got phosphorylated and activated in HCV-infected cells. The JNK inhibitor SP600125 clearly prevented the phosphorylation of c-Jun, and concomitantly recovered the suppression of FoxO1 phosphorylation in HCV-infected cells, suggesting that HCV activates the JNK/c-Jun signaling pathway, resulting in the nuclear accumulation of FoxO1 by reducing its phosphorylation status. The detailed mechanisms of HCV-induced suppression of FoxO1 phosphorylation via the JNK/c-Jun signaling pathway remain to be explored. There are at least two possibilities. The JNK/c-Jun signaling pathway (1) suppresses a protein kinase, or (2) activates a protein phosphatase to reduce phosphorylation of FoxO1.

HCV-INDUCED MITOCHONDRIAL REACTIVE OXYGEN SPECIES PRODUCTION IS INVOLVED IN INCREASED GLUCOSE PRODUCTION THROUGH JNK ACTIVATION

Hepatitis C virus infection increases mitochondrial reactive oxygen species (ROS) production (Deng et al., 2008). *N*-acetyl cysteine (NAC; a general antioxidant) clearly prevented the phosphorylation of JNK, and concomitantly canceled the suppression of FoxO1 phosphorylation in HCV-infected cells, suggesting that

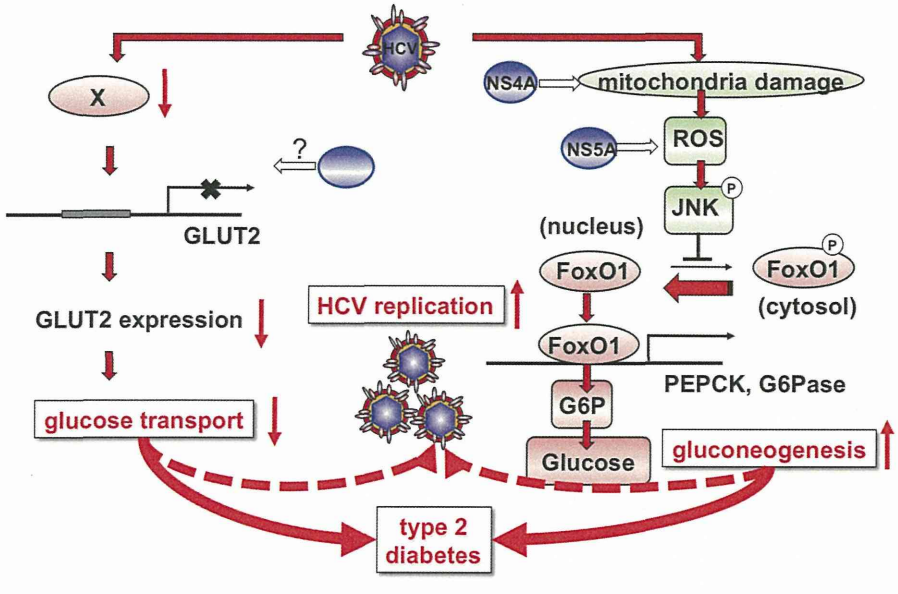

FIGURE 2 | A proposed mechanism of HCV-induced glucose metabolic disorders. HCV infection down-regulates cell surface expression of GLUT2 in hepatocytes at the transcriptional level. HCV down-regulates a transcription factor involved in GLUT2 gene expression through an unknown mechanism. HCV infection induces mitochondria damage and ROS production, leading to JNK activation. HCV NS4A protein is involved in mitochondrial damage. HCV NS5A protein is involved in ROS production. HCV-induced ROS production causes JNK activation, resulting in the decreased phosphorylation and nuclear accumulation of FoxO1. Nuclear accumulation of FoxO1 up-regulates gene expression of PEPCK and G6Pase, leading eventually to increased glucose production by gluconeogenesis. High glucose levels in the hepatocytes may confer an advantage in efficient replication of HCV.

HCV-induced ROS production is involved in the JNK activation. There was no significant difference in HCV RNA replication or infectious virus release between SP600125- or NAC-treated HCV-infected cells and non-treated HCV-infected cells. These results suggest that ROS-mediated JNK activation plays a key role in the suppression of FoxO1 phosphorylation, nuclear accumulation of FoxO1, and enhancement of glucose production in HCV-infected cells (Deng et al., 2011).

HCV NS5A IS INVOLVED IN THE ENHANCEMENT OF GLUCOSE PRODUCTION

Then we sought to determine which HCV protein(s) is involved in the enhancement of glucose production. Transient expression of NS5A protein in Huh-7.5 cells significantly promoted the gene expression levels of G6Pase and PEPCK determined by real time quantitative RT-PCR. Promoter assay revealed that the level of PEPCK promoter activity was significantly higher in NS5A-expressing cells than in the control cells. Our results suggest that NS5A activate both the PEPCK promoter and the G6Pase promoter, leading to an increase in glucose production (Deng et al., 2011). The study by Banerjee et al. (2010) suggests that the HCV core protein modulates FoxO1 and FoxA2 activation and affects insulin-induced metabolic gene regulation in human hepatocytes. Our results, however, suggest that the HCV core protein is not significantly involved in the increased gluconeogenesis (Deng et al., 2011). The difference between these two studies needs to be explored.

There were previous reports suggesting that ROS production is induced in NS5A-expressing cells (Dionisio et al., 2009) or in hepatocytes of NS5A transgenic mice (Wang et al., 2009). We therefore sought to determine whether NS5A contributes to increased hepatic gluconeogenesis through the induction of ROS production. NS5A-expressing cells displayed a much stronger signal of ROS than in control cells. NS5A-expressing cells promoted phosphorylation level at Ser63 of c-Jun and suppressed FoxO1 phosphorylation at Ser319, suggesting that NS5A mediates JNK/c-Jun activation and FoxO1 phosphorylation suppression. These results suggest that NS5A play a role in the HCV-induced enhancement of hepatic gluconeogenesis through JNK/c-Jun activation and FoxO1 phosphorylation suppression.

CONCLUSION AND FUTURE PERSPECTIVES

Taken together, we propose a model of HCV-induced glucose metabolic disorders as shown in **Figure 2**. HCV infection down-regulates cell surface expression of GLUT2 in hepatocytes at the transcriptional level. HCV down-regulates a transcription factor involved in GLUT2 gene expression through an unknown mechanism. As GLUT2 is a facilitative GLUT, it ensures large bidirectional fluxes of glucose in and out the cell due to its low affinity and high capacity (Leturque et al., 2009). Down-regulated cell surface expression of GLUT2 results in disruption of bidirectional transport of glucose in hepatocytes. Even in the fasting state, down-regulation of GLUT2 may result in low glucose uptake of hepatocytes, causing hyperglycemia. In the fed state, glucose secretion from hepatocytes may be suppressed due to low level cell surface expression of GLUT2, as GLUT2 is a bidirectional transporter.

Hepatitis C virus infection induces mitochondria damage and ROS production, leading to JNK activation. HCV NS4A protein is involved in mitochondrial damage (Nomura-Takigawa et al., 2006). HCV NS5A protein is involved in ROS production (Dionisio et al., 2009; Wang et al., 2009; Deng et al., 2011). HCV-induced ROS production causes JNK activation, which results in the decreased phosphorylation and nuclear accumulation of FoxO1 by an unidentified mechanism. Nuclear accumulation of FoxO1 up-regulates gene expression of PEPCK and G6Pase, leading eventually to increased glucose production by gluconeogenesis (Deng et al., 2011).

These two pathways, HCV-induced down-regulation of GLUT2 expression and up-regulation of gluconeogenesis, may contribute to development of type 2 diabetes in HCV-infected patients at least to some extent. HCV-induced down-regulation of GLUT2 expression and up-regulation of gluconeogenesis may result in high concentration of glucose in HCV-infected hepatocytes. As suggested in a recent study, low glucose concentration in the hepatocytes inhibits HCV replication (Nakashima et al., 2011). Therefore, high glucose levels in the hepatocytes may confer an advantage in efficient replication of HCV.

Our understanding of HCV-induced glucose metabolic disorders will require much more work to fully unfold this pathway. Further investigation including the mechanism of HCV-induced GLUT2 downregualtion, JNK-mediated decreased phosphorylation of FoxO1, and the possible effect(s) of the dysregulation of hepatic gluconeogenesis on the HCV life cycle and host cells are currently under way.

ACKNOWLEDGMENTS

The authors are grateful to all of their co-workers who contributed to the studies cited here. This work was supported in part by grants-in-aid for Research on Hepatitis from the Ministry of Health, Labor and Welfare, Japan, and the Japan Initiative for Global Research Network on Infectious Diseases (J-GRID) program of Ministry of Education, Culture, Sports, Science and Technology, Japan. This study was also carried out as part of the Global Center of Excellence program of Kobe University Graduate School of Medicine, and the Science and Technology Research Partnership for Sustainable Development (SATREPS) program of Japan Science and Technology Agency (JST) and Japan International Cooperation Agency (JICA).

REFERENCES

Banerjee, A., Meyer, K., Mazumdar, B., Ray, R. B., and Ray, R. (2010). Hepatitis C virus differentially modulates activation of forkhead transcription factors and insulin-induced metabolic gene expression. *J. Virol.* 84, 5936–5946.

Bungyoku, Y., Shoji, I., Makine, T., Adachi, T., Hayashida, K., Nagano-Fujii, M., Ide, Y. H., Deng, L., and Hotta, H. (2009). Efficient production of infectious hepatitis C virus with adaptive mutations in cultured hepatoma cells. *J. Gen. Virol.* 90, 1681–1691.

Burdette, D., Olivarez, M., and Waris, G. (2010). Activation of transcription factor Nrf2 by hepatitis C virus induces the cell-survival pathway. *J. Gen. Virol.* 91, 681–690.

Choo, Q. L., Richman, K. H., Han, J. H., Berger, K., Lee, C., Dong, C., Gallegos, C., Coit, D., Medina-Selby,

R., Barr, P. J., Weiner, A. J., Bradley, D. W., Kuo, G., and Houghton, M. (1991). Genetic organization and diversity of the hepatitis C virus. *Proc. Natl. Acad. Sci. U.S.A.* 88, 2451–2455.

Clore, J. N., Stillman, J., and Sugerman, H. (2000). Glucose-6-phosphatase flux in vitro is increased in type 2 diabetes. *Diabetes* 49, 969–974.

Deng, L., Adachi, T., Kitayama, K., Bungyoku, Y., Kitazawa, S., Ishido, S., Shoji, I., and Hotta, H. (2008). Hepatitis C virus infection induces apoptosis through a Bax-triggered, mitochondrion-mediated, caspase 3-dependent pathway. *J. Virol.* 82, 10375–10385.

Deng, L., Shoji, I., Ogawa, W., Kaneda, S., Soga, T., Jiang, D. P., Ide, Y. H., and Hotta, H. (2011). Hepatitis C virus infection promotes hepatic gluconeogenesis through an NS5A-mediated, FoxO1-dependent pathway. *J. Virol.* 85, 8556–8568.

Dionisio, N., Garcia-Mediavilla, M. V., Sanchez-Campos, S., Majano, P. L., Benedicto, I., Rosado, J. A., Salido, G. M., and Gonzalez-Gallego, J. (2009). Hepatitis C virus NS5A and core proteins induce oxidative stress-mediated calcium signalling alterations in hepatocytes. *J. Hepatol.* 50, 872–882.

Godoy, A., Ulloa, V., Rodriguez, F., Reinicke, K., Yanez, A. J., Garcia Mde, L., Medina, R. A., Carrasco, M., Barberis, S., Castro, T., Martinez, F., Koch, X., Vera, J. C., Poblete, M. T., Figueroa, C. D., Peruzzo, B., Perez, F., and Nualart, F. (2006). Differential subcellular distribution of glucose transporters GLUT1-6 and GLUT9 in human cancer: ultrastructural localization of GLUT1 and GLUT5 in breast tumor tissues. *J. Cell. Physiol.* 207, 614–627.

Gross, D. N., van den Heuvel, A. P., and Birnbaum, M. J. (2008). The role of FoxO in the regulation of metabolism. *Oncogene* 27, 2320–2336.

Hirota, K., Sakamaki, J., Ishida, J., Shimamoto, Y., Nishihara, S., Kodama, N., Ohta, K., Yamamoto, M., Tanimoto, K., and Fukamizu, A. (2008). A combination of HNF-4 and Foxo1 is required for reciprocal transcriptional regulation of glucokinase and glucose-6-phosphatase genes in response to fasting and feeding. *J. Biol. Chem.* 283, 32432–32441.

Karpac, J., and Jasper, H. (2009). Insulin and JNK: optimizing metabolic homeostasis and lifespan. *Trends Endocrinol. Metab.* 20, 100–106.

Kasai, D., Adachi, T., Deng, L., Nagano-Fujii, M., Sada, K., Ikeda, M., Kato, N., Ide, Y. H., Shoji, I., and Hotta, H. (2009). HCV replication suppresses cellular glucose uptake through down-regulation of cell surface expression of glucose transporters. *J. Hepatol.* 50, 883–894.

Kawaguchi, T., Yoshida, T., Harada, M., Hisamoto, T., Nagao, Y., Ide, T., Taniguchi, E., Kumemura, H., Hanada, S., Maeyama, M., Baba, S., Koga, H., Kumashiro, R., Ueno, T., Ogata, H., Yoshimura, A., and Sata, M. (2004). Hepatitis C virus down-regulates insulin receptor substrates 1 and 2 through up-regulation of suppressor of cytokine signaling 3. *Am. J. Pathol.* 165, 1499–1508.

Koike, K. (2007). Hepatitis C virus contributes to hepatocarcinogenesis by modulating metabolic and intracellular signaling pathways. *J. Gastroenterol. Hepatol.* 22(Suppl. 1), S108–S111.

Lemon, S. M., Walker, C., Alter, M. J., and Yi, M. (2007). "Hepatitis C virus," in *Fields' Virology*, 5th Edn, eds B. N. Fields, D. M. Knipe, and P. M. Howley (Philadelphia, PA: Wolters Kluwer Health/Lippincott Williams and Wilkins), 1291–1304.

Leturque, A., Brot-Laroche, E., and Le Gall, M. (2009). GLUT2 mutations, translocation, and receptor function in diet sugar managing. *Am. J. Physiol. Endocrinol. Metab.* 296, E985–E992.

Lindenbach, B. D., Evans, M. J., Syder, A. J., Wolk, B., Tellinghuisen, T. L., Liu, C. C., Maruyama, T., Hynes, R. O., Burton, D. R., McKeating, J. A., and Rice, C. M. (2005). Complete replication of hepatitis C virus in cell culture. *Science* 309, 623–626.

Lohmann, V., Korner, F., Koch, J., Herian, U., Theilmann, L., and Bartenschlager, R. (1999). Replication of subgenomic hepatitis C virus RNAs in a hepatoma cell line. *Science* 285, 110–113.

Macheda, M. L., Rogers, S., and Best, J. D. (2005). Molecular and cellular regulation of glucose transporter (GLUT) proteins in cancer. *J. Cell. Physiol.* 202, 654–662.

Mason, A. L., Lau, J. Y., Hoang, N., Qian, K., Alexander, G. J., Xu, L., Guo, L., Jacob, S., Regenstein, F. G., Zimmerman, R., Everhart, J. E., Wasserfall, C., Maclaren, N. K., and Perrillo, R. P. (1999). Association of diabetes mellitus and chronic hepatitis C virus infection. *Hepatology* 29, 328–333.

Miyamoto, H., Moriishi, K., Moriya, K., Murata, S., Tanaka, K., Suzuki, T., Miyamura, T., Koike, K., and Matsuura, Y. (2007). Involvement of the PA28gamma-dependent pathway in insulin resistance induced by hepatitis C virus core protein. *J. Virol.* 81, 1727–1735.

Nakashima, K., Takeuchi, K., Chihara, K., Hotta, H., and Sada, K. (2011). Inhibition of hepatitis C virus replication through adenosine monophosphate-activated protein kinase-dependent and -independent pathways. *Microbiol. Immunol.* 55, 774–782.

Negro, F. (2011). Mechanisms of hepatitis C virus-related insulin resistance. *Clin. Res. Hepatol. Gastroenterol.* 35, 358–363.

Negro, F., and Alaei, M. (2009). Hepatitis C virus and type 2 diabetes. *World J. Gastroenterol.* 15, 1537–1547.

Nomura-Takigawa, Y., Nagano-Fujii, M., Deng, L., Kitazawa, S., Ishido, S., Sada, K., and Hotta, H. (2006). Non-structural protein 4A of Hepatitis C virus accumulates on mitochondria and renders the cells prone to undergoing mitochondria-mediated apoptosis. *J. Gen. Virol.* 87, 1935–1945.

Pazienza, V., Clement, S., Pugnale, P., Conzelman, S., Foti, M., Mangia, A., and Negro, F. (2007). The hepatitis C virus core protein of genotypes 3a and 1b downregulates insulin receptor substrate 1 through genotype-specific mechanisms. *Hepatology* 45, 1164–1171.

Poynard, T., Yuen, M. F., Ratziu, V., and Lai, C. L. (2003). Viral hepatitis C. *Lancet* 362, 2095–2100.

Rozance, P. J., Limesand, S. W., Barry, J. S., Brown, L. D., Thorn, S. R., LoTurco, D., Regnault, T. R., Friedman, J. E. and Hay, W. W. Jr. (2008). Chronic late-gestation hypoglycemia upregulates hepatic PEPCK associated with increased PGC1alpha mRNA and phosphorylated CREB in fetal sheep. *Am. J. Physiol. Endocrinol. Metab.* 294, E365–E370.

Shintani, Y., Fujie, H., Miyoshi, H., Tsutsumi, T., Tsukamoto, K., Kimura, S., Moriya, K., and Koike, K. (2004). Hepatitis C virus infection and diabetes: direct involvement of the virus in the development of insulin resistance. *Gastroenterology* 126, 840–848.

Takashima, M., Ogawa, W., Hayashi, K., Inoue, H., Kinoshita, S., Okamoto, Y., Sakaue, H., Wataoka, Y., Emi, A., Senga, Y., Matsuki, Y., Watanabe, E., Hiramatsu, R., and Kasuga, M. (2010). Role of KLF15 in regulation of hepatic gluconeogenesis and metformin action. *Diabetes* 59, 1608–1615.

Tzivion, G., Dobson, M., and Ramakrishnan, G. (2011). FoxO transcription factors; Regulation by AKT and 14-3-3 proteins. *Biochim. Biophys. Acta* 1813, 1938–1945.

van der Horst, A., and Burgering, B. M. (2007). Stressing the role of FoxO proteins in lifespan and disease. *Nat. Rev. Mol. Cell Biol.* 8, 440–450.

Wakita, T., Pietschmann, T., Kato, T., Date, T., Miyamoto, M., Zhao, Z., Murthy, K., Habermann, A., Krausslich, H. G., Mizokami, M., Bartenschlager, R., and Liang, T. J. (2005). Production of infectious hepatitis C virus in tissue culture from a cloned viral genome. *Nat. Med.* 11, 791–796.

Wang, A. G., Lee, D. S., Moon, H. B., Kim, J. M., Cho, K. H., Choi, S. H., Ha, H. L., Han, Y. H., Kim, D. G., Hwang, S. B., and Yu, D. Y. (2009). Non-structural 5A protein of hepatitis C virus induces a range of liver pathology in transgenic mice. *J. Pathol.* 219, 253–262.

Wu, X., and Freeze, H. H. (2002). GLUT14, a duplicon of GLUT3, is specifically expressed in testis as alternative splice forms. *Genomics* 80, 553–557.

Zhao, X., Gan, L., Pan, H., Kan, D., Majeski, M., Adam, S. A., and Unterman, T. G. (2004). Multiple elements regulate nuclear/cytoplasmic shuttling of FOXO1: characterization of phosphorylation- and 14-3-3-dependent and -independent mechanisms. *Biochem. J.* 378, 839–849.

Conflict of Interest Statement: The authors declare that the research was conducted in the absence of any commercial or financial relationships that could be construed as a potential conflict of interest.

Received: 01 December 2011; accepted: 25 December 2011; published online: 10 January 2012.

Citation: Shoji I, Deng L and Hotta H (2012) Molecular mechanism of hepatitis C virus-induced glucose metabolic disorders. Front. Microbio. 2:278. doi: 10.3389/fmicb.2011.00278

This article was submitted to Frontiers in Virology, a specialty of Frontiers in Microbiology.

Copyright © 2012 Shoji, Deng and Hotta. This is an open-access article distributed under the terms of the Creative Commons Attribution Non Commercial License, which permits non-commercial use, distribution, and reproduction in other forums, provided the original authors and source are credited.

OPEN ACCESS Freely available online

PLOS ONE

HCV NS5A Protein Containing Potential Ligands for Both Src Homology 2 and 3 Domains Enhances Autophosphorylation of Src Family Kinase Fyn in B Cells

Kenji Nakashima[1], Kenji Takeuchi[1,2], Kazuyasu Chihara[1,2], Tomoko Horiguchi[1], Xuedong Sun[1], Lin Deng[3], Ikuo Shoji[3], Hak Hotta[3], Kiyonao Sada[1,2]*

1 Division of Genome Science and Microbiology, Department of Pathological Sciences, School of Medicine, Faculty of Medical Sciences, University of Fukui, Eiheiji, Japan, **2** Organization for Life Science Advancement Programs, University of Fukui, Eiheiji, Japan, **3** Division of Microbiology, Center for Infectious Diseases, Kobe University Graduate School of Medicine, Kobe, Japan

Abstract

Hepatitis C virus (HCV) infects B lymphocytes and induces mixed cryoglobulinemia and B cell non-Hodgkin's lymphoma. The molecular mechanism for the pathogenesis of HCV infection-mediated B cell disorders remains obscure. To identify the possible role for HCV nonstructural 5A (NS5A) protein in B cells, we generated the stable B cell lines expressing Myc-His tagged NS5A. Immunoprecipitation study in the presence or absence of pervanadate (PV) implied that NS5A was tyrosine phosphorylated by pervanadate (PV) treatment of the cells. Therefore we examined pull-down assay by using glutathione S-transferase (GST)-fusion proteins of various Src homology 2 (SH2) domains, which associates with phosphotyrosine within a specific amino acid sequence. The results showed that NS5A specifically bound to SH2 domain of Fyn from PV-treated B cells in addition to Src homology 3 (SH3) domain. Substitution of Arg^{176} to Lys in the SH2 domain of Fyn abrogated this interaction. Deletion mutational analysis demonstrated that N-terminal region of NS5A was not required for the interaction with the SH2 domain of Fyn. Tyr^{334} was identified as a tyrosine phosphorylation site in NS5A. Far-western analysis revealed that SH2 domain of Fyn directly bound to NS5A. Fyn and NS5A were colocalized in the lipid raft. These results suggest that NS5A directly binds to the SH2 domain of Fyn in a tyrosine phosphorylation-dependent manner. Lastly, we showed that the expression of NS5A in B cells increased phosphorylation of activation loop tyrosine in the kinase domain of Fyn. NS5A containing ligand for both SH2 and SH3 domains enhances an aberrant autophosphorylation and kinase activity of Fyn in B cells.

Citation: Nakashima K, Takeuchi K, Chihara K, Horiguchi T, Sun X, et al. (2012) HCV NS5A Protein Containing Potential Ligands for Both Src Homology 2 and 3 Domains Enhances Autophosphorylation of Src Family Kinase Fyn in B Cells. PLoS ONE 7(10): e46634. doi:10.1371/journal.pone.0046634

Editor: Philippe Gallay, Scripps Research Institute, United States of America

Received April 12, 2012; **Accepted** September 2, 2012; **Published** October 16, 2012

Copyright: © 2012 Nakashima et al. This is an open-access article distributed under the terms of the Creative Commons Attribution License, which permits unrestricted use, distribution, and reproduction in any medium, provided the original author and source are credited.

Funding: This study was supported in part by research funding from the University of Fukui, Takeda Science Foundation, Yakult Foundation, and the Grant-in-Aids from the Japan Society for the Promotion of Science and the Ministry of Education, Culture, Sports and Technology, Japan. The funders had no role in study design, data collection and analysis, decision to publish, or preparation of the manuscript.

Competing Interests: The authors have declared that no competing interests exist.

* E-mail: ksada@u-fukui.ac.jp

Introduction

HCV is a small enveloped positive-sense RNA virus classified within the family *Flaviviridae* [1,2]. In addition to liver cells, HCV infects B cells, leading to mixed cryoglobulinemia and B cell non-Hodgkin's lymphoma [3–5]. HCV infection in B cells enhances the expression of lymphomagenesis-related genes, such as activation-induced cytidine deaminase (AID) [6,7]. However, the molecular mechanisms of HCV infection-mediated B cell disorders remain elusive.

Non-receptor type of protein-tyrosine kinase Fyn is a member of the Src family kinases, and has regulatory roles in immune receptor signaling. Recently, Fyn has been recognized as an important mediator of mitogenic signaling and regulator of cell cycle entry, growth and proliferation. As for pathological aspects, Fyn is overexpressed in various cancers, and overexpression of Fyn in cultured cells resulted in cancer-like phenotypes [8].

The Src family kinases all share a common structure and pattern of activation. The domains of these proteins include SH2, SH3, and kinase domains followed by a short C-terminal regulatory tail. The SH2 and SH3 domains are highly conserved regions and mediate protein-protein interactions: the SH2 domain binds to phosphotyrosine residue within the specific amino acid sequence, while the SH3 domain recognizes proline rich regions. HCV NS5A was shown to interact with various SH3 domains of intracellular signaling molecules, and the kinase activity of Fyn was upregulated in liver cell lines harboring HCV replicon [9]. Binding of ligands to both the SH2 and SH3 domains disrupts autoinhibitory intramolecular interactions and leads to the opened conformation. Then autophosphorylation of the activation loop tyrosine (Tyr^{420} in Fyn) and dephosphorylation of the C-terminal tail (Tyr^{531} in Fyn) by protein-tyrosine phosphatases lead to the activation of kinase activity [10].

Previously, we reported that Syk, another non-receptor type of protein-tyrosine kinase interacts with transiently expressed NS5A in PV treated BJAB B cells [11]. This suggested that protein-tyrosine phosphorylation is required for the association of NS5A with Syk, because PV is a nonspecific inhibitor of protein-tyrosine phosphatases and treatment of cells with PV causes increase in

protein-tyrosine phosphorylation in whole cells. Recently Pfannkuche *et al.* reported that NS5A binds to the SH2 domain of Src [12]. However, molecular mechanism of their interaction and effect of NS5A on the kinase activity of Src remain unclear.

In this study, we investigated the interaction between NS5A and the SH2 domain of Fyn in B cells.

Materials and Methods

Antibodies and cDNAs

Anti-NS5A and anti-glyceraldehyde-3-phosphate dehydrogenase (GAPDH) mAbs were purchased from Millipore (Bedford, MA, USA). Anti-Myc mAb and anti-Fyn antibody were obtained from Santa Cruz Biotechnology (Santa Cruz, CA, USA). Anti-phosphotyrosine (pTyr) (PY20) and human anti-IgM mAbs were from Zymed (South San Francisco, CA, USA). Anti-GST mAb was from Nacalai (Kyoto, Japan). Anti-phospho-Src family (Tyr416) antibody, which detects phosphorylated amount of Tyr^{420} in Fyn, was from Cell Signaling Technology (Danvers, MA, USA). The pEF1A-NS5A(Con1)-Myc-His plasmid and its deletion or substitution mutants were described previously [11]. Deletion of NS5A 127–146 (NS5A Δ127–146) was generated by the PCR-based method using four primers, 5′-TTGGTACCATGTCCGGCTCGTGGCTAAGAG-3′, 5′-GCTCTAGAGCAGCAGACGACGTCCTCA-3′, 5′-GGTTACGCGGGTGGGGGATCCCGAATTCTTCACAGAAGTG-3′, and 5′-CACTTCTGTGAAGAATTCGGGATCCCCCACCCGCGTAACC-3′, using NS5A cDNA as a template. Substitution of Tyr^{129} to Phe (Y129F) of NS5A 1–146 was generated by the site-directed mutagenesis using two primers, 5′-GGGGATTTCCACTTCGTGACGGGCA-3′ and 5′-TGCCCGTCACGAAGTGGAAATCCCC-3′, using NS5A 1–146 cDNA as a template. Substitutions of Tyr^{182} to Phe (Y182F), Tyr^{321} to Phe (Y321F), and Tyr^{334} to Phe (Y334F) of NS5A 147–447 were generated by the site-directed mutagenesis using two specific primers designed by QuikChange Primer Design Program (www.genomics.agilent.com), using NS5A 147–447 as a template. The resulted mutations were confirmed by the DNA sequencing.

Cell culture and transfection

B-lymphoid leukemia BJAB cells were kindly provided from Dr. Satoshi Ishido (RIKEN, Yokohama, Japan) [13] and maintained as described previously [14]. For the stable transfection of BJAB cells, 6 μg of linearized pEF1A-NS5A(Con1)-Myc-His was transfected into 5×10^6 cells/500 μl of cells by electroporation (240 V, 950 μF). Stably transfected cell lines were selected with 0.4 mg/ml of active G418 (Wako, Osaka, Japan) [15]. Cell lines were screened by level of protein expression by immunoblotting of detergent soluble lysates with anti-NS5A and anti-GAPDH mAbs as an internal control. Two positive cloned lines were selected for further analysis. For control cells, linearized empty vector was transfected by electroporation, and pooled clones resistant to 0.4 mg/ml of active G418 were utilized as control cells. COS cells were obtained from American Type Culture Collection (Manassas, VA, USA) and Ramos-T cells were kindly provided from Dr. Hamid Band (Nebraska Medical Center, NE, USA) [16]. Transient transfection of COS cells and Ramos-T cells were described previously [17]. Huh-7.5 cells were kindly provided from Dr. Charles M. Rice (The Rockefeller University, NY, USA) [18] and stably harboring an HCV replicon (pFK5B/2884 Gly) were described previously [11].

Cell activation, immunoprecipitation and immunoblotting

BJAB cells (10^8) were washed twice with serum free medium and treated with 100 μM PV or 10 μg/ml of anti-IgM mAb for 3 min at 37°C in the same medium. Either unstimulated or stimulated cells were washed twice with ice-cold PBS and then solubilized in the lysis buffer (1% Triton X-100, 50 mM Tris, pH7.4, 150 mM NaCl, 10 mM EDTA, 100 mM NaF, 1 mM Na_3VO_4, 1 mM phenylmethylsulfonyl fluoride and 2 μg/ml aprotinin) on ice. In some experiments, 0.5% Nonidet P-40 was used instead of 1% Triton. Precleared cell lysates were incubated with the indicated antibodies prebound to protein A-agarose beads (Sigma, St. Louis, MO, USA). After rotation for 90 min at 4°C, the beads were washed 4 times with the lysis buffer, and the immunoprecipitated proteins were eluted by the heat treatment for 5 min at 100°C with 2×sampling buffer. Precipitated proteins or cell lysates were separated by SDS-PAGE and transferred to polyvinylidene difluoride (PVDF) membrane (Millipore). After blocking in 5% milk in TBST (25 mM Tris, pH 8.0, 150 mM NaCl, and 0.1% Tween 20), the blots were incubated with the primary antibodies and then horseradish peroxidase-conjugated goat anti-rabbit IgG, goat anti-mouse IgG antibodies (Jackson ImmunoResearch Laboratories, West Grove, PA, USA), or horseradish peroxidase-conjugated protein G (Sigma) in TBST. To enhance the signals, Immuno-enhancer Reagent A (Wako) was utilized in the reaction with anti-pTyr (pY20) mAb. Finally, proteins were visualized by the enhanced chemiluminescence (ECL) reagent (Western Lightning, PerkinElmer Life Sciences, Boston, MA) [19]. Immunoblot quantification was performed using the program Scion Image (Scion, Frederick, MD, USA).

Pull-down assay

The cDNA for Fyn-SH2 (Trp^{149}-Ala^{257}) and –SH3 (Thr^{82}-Glu^{148}) were amplified by PCR using paired primers 5′-GGAATTCATGGTACTTTGGAAAACTTGGC-3′ and 5′-CCGCTCGAGATCTTTAGCCAATCCAGAAGT-3′ for –SH2, 5′-GGAATTCAACAGGAGTGACACTGTTTGTG-3′ and 5′-CCGCTCGAGCTCTTCTGCCTGGATGGAGTC-3′ for –SH3, using mouse Fyn(T) cDNA (a gift from Dr. Yasuhiro Minami, Kobe University, Kobe, Japan) as a template. The cDNA for c-Abl-SH2 (Typ^{146}-His^{221}) and -SH3 (Leu^{84}-Val^{138}) were amplified by PCR using paired primers 5′-CGGAATTCCTGGTATCATGGCCCTGTATCT-3′ and 5′-ATAGTTTAGCGGCCGCTAGCTGGGTAGTGGAGTGTGGT-3′ for -SH2, 5′-CGGAATTCCCTTTTTGTGGCACTCTATGAT-3′ and 5′-TAGTTTAGCGGCCGCTGACGGGGGTGATGTAGTTGCT-3′ for -SH3, using mouse c-Abl cDNA (a gift from Dr. David Baltimore, California Institute of Technology, CA, USA) as a template. The cDNA for Cbl-b N-terminal region containing SH2 domain (Ala^2-Pro^{349}) was amplified by PCR using 5′-CGGAATTCCGCAAACTCAATGAATGGCAGA-3′ and 5′-CCGCTCGAGCTAAGGTGTAGGTTCACATAATCC-3′, using human Cbl-b cDNA (a gift form Dr. Stanley Lipkowitz, National Naval Cancer Center, MD, USA) as a template. Resulted PCR fragments were subcloned into pGEX-4T.3 (GE Healthcare, Piscataway, NJ, USA) to make domain in-frame with the downstream of GST and verified by DNA sequencing. The GST-rat Lyn-SH2 and Syk-SH2 (N+C) expression constructs were provided by Dr. Reuben P. Siraganian (National Institutes of Health, MD, USA). Preparation of GST-rat Vav1-SH2, mouse c-Abl SH3 domain-binding protein-2 (3BP2)-SH2, human phospholipase C (PLC)-γ2-SH2 (N+C), and rat Lyn-SH3 domain expression constructs were described elsewhere [17,20,21]. Substitution of Arg^{176} to Lys (R176K) by a point mutation of pGEX-

4T.3-Fyn-SH2 was generated by the site-directed mutagenesis using two primers 5′-TCAAAGAGAGCCAAACCACCAAAGG-3′ and 5′-TAAGAAAGGTACCTCTTGGGTTTCC-3′, using Fyn-SH2 cDNA wild type as a template. The resulted point mutation was confirmed by the DNA sequencing. All these SH2 and SH3 domains were fused downstream of GST. The GST fusion proteins were affinity-purified with glutathione Sepharose 4B beads (GE Healthcare). Extraction of GST-fusion proteins from bacteria was confirmed by the SDS-PAGE and Coomassie brilliant blue staining [22].

BJAB cells (10^8), Huh-7.5 cells stably harboring an HCV replicon (3×10^6), COS cells (10^6) or Ramos B cells expressing SV40 T antigen (Ramos-T cells) (10^7) were washed twice with serum free medium and stimulated with 100 μM PV for 3 min at 37°C. Either unstimulated or stimulated cells were solubilized in the binding buffer (1% NP-40, 50 mM Tris, pH7.4, 150 mM NaCl, 10 mM EDTA, 100 mM NaF, 1 mM Na_3VO_4, 1 mM phenylmethylsulfonyl fluoride and 2 μg/ml aprotinin). After centrifugation, the resulted supernatants were reacted with 20 μg of GST-fusion proteins prebound to glutathione Sepharose 4B beads for 90 min at 4°C. The beads were washed 4 times with the binding buffer. Proteins interacting with GST-fusion proteins were eluted by heat treatment for 5 min at 100°C with 2×sampling buffer, separated by SDS-PAGE, and analyzed by immunoblotting.

Far-western

Anti-NS5A immunoprecipitates from BJAB cells (3×10^7) were separated by SDS-PAGE and transferred to PVDF membrane. After blocking, the membranes were incubated with 2.5 μg/ml of GST or GST-Fyn-SH2 for 1 h at 4°C. After extensive washing, membranes were reacted with anti-GST mAb, subsequently reacted with horseradish peroxidase conjugated goat anti-mouse IgG antibody, and then subjected to ECL detection [17].

Subcellular fractionation

The low density detergent-insoluble fractions were prepared by sucrose density gradient centrifugation as described [23]. BJAB cells (10^8) were solubilized in 2.5 ml of 0.05% Triton in MNEV buffer (150 mM NaCl, 25 mM Mes, pH 6.5, 5 mM EDTA, 1 mM Na_3VO_4, and protease inhibitors) and dounced 10 times. Homogenates were cleared of intact cells by centrifugation for 10 minutes at 200 *g*. The resultant supernatants (2.4 ml) were mixed with equal volumes of 80% sucrose in MNEV buffer (final, 40% sucrose and 0.025% Triton), overlayered by 4.8 ml 30% and 2.4 ml 5% sucrose in MNEV buffer, and then centrifuged for 20 hours at 200 000 *g* (P40ST rotor, Himac CP80WX, Hitachi, Tokyo, Japan). After sucrose density gradient centrifugation, 9 fractions were collected from the top of the gradient and analyzed by the immunoblotting.

Statistical analysis

Quantification of Fyn was analyzed by ImageJ software. The two-tailed Student t-test was applied to evaluate the statistical significance of differences found. A P value of <0.05 was considered statistically significant.

In vitro kinase assay

Unstimulated BJAB cells were washed twice with ice-cold PBS and then solubilized in the lysis buffer. Precleared cell lysates were incubated with anti-Fyn antibody prebound to protein A-agarose beads. After rotation for 90 min at 4°C, the beads were washed 4 times with the lysis buffer, 2 times with the kinase buffer without ATP, then incubated with 20 μl of the kinase buffer (40 mM Hepes, pH 7.5, 10 mM $MgCl_2$, 2 mM $MnCl_2$, 4 μM ATP, 4 μCi [γ-^{32}P] ATP) and 2.5 μg of acid-treated enolase (Sigma) for 30 min at room temperature. Reaction was terminated and proteins were eluted by the heat treatment for 5 min at 100°C with 2×sampling buffer. Proteins were separated by SDS-PAGE and gel was incubated with 1N KOH for 1 h at 56°C to remove phosphoserine and most of phosphothreonine. After fixation, the gel was dried and radiolabeled proteins were visualized by autoradiography. Immunoprecipitation of Fyn was confirmed by the immunoblotting.

Results

HCV NS5A associates with the SH2 domain of Fyn

To identify HCV NS5A-interacting protein in B cells, we generated the stable B cell lines in which Myc-His tagged NS5A protein is constitutively expressed. Since we confirmed that the parental cells did not express NS5A, we choose the clones in which the level of NS5A expression was highest (Fig. 1A). In the following experiments, two cloned lines (clone 3 and 7) were examined, although some figures present the results from only one representative cell line. For control, vector plasmid was transfected into the same parental cells and G418-resistant clones were pooled and utilized as control cells.

Next, we performed immunoprecipitation study using anti-Myc mAb and found tyrosine phosphorylated proteins (Fig. 1B). This suggests that NS5A was tyrosine phosphorylated by PV treatment or another protein with similar size that associates with NS5A (Fig. 1B). Another experiment by affinity tag purification using Nickel column which could react with His-tag (His-Accept kit, Nacalai) also showed some tyrosine phosphorylated proteins in NS5A protein complex (data not shown). These findings suggest the possible involvement of protein-tyrosine phosphorylation associating with NS5A. Therefore, we tried to identify the protein which associates with NS5A through SH2 domain, which recognizes specific phosphotyrosine-containing amino acid sequence.

Then we carried out pull-down assay using GST-fusion proteins of various SH2 domains (Fig. 1C). Among these, the SH2 domain of Fyn dramatically bound to NS5A from PV-treated B cells. The SH2 domains of PLC-γ2 weakly bound to NS5A. The SH2 domains of Lyn, Abl, Vav, 3BP2, Syk or Cbl-b interacted with NS5A at very low level (long exposure, data not shown). GST-Lyn-SH3 was utilized as positive control because it was reported to interact with NS5A [9]. Therefore, this data demonstrated that HCV NS5A selectively binds to the SH2 domains of Fyn and PLC-γ2 in B cells. GST-human Fyn-SH2 also interacted with NS5A (Fig. S1). Moreover, the NS5A interaction with GST-Fyn-SH2 was observed even in the context of HCV RNA replication (Fig. 1D). Thus, HCV NS5A selectively associates with the SH2 domain of Fyn.

NS5A binds to the SH2 domain of Fyn in a tyrosine phosphorylation-dependent manner

PV treatment of cells dramatically enhances the binding of NS5A to the SH2 domain of Fyn, but not with that of Lyn or Abl (Fig. 2A). Substitution of Arg^{176} to Lys in the SH2 domain of Fyn, which caused the loss of association with phosphotyrosine residue, abrogated the binding of the SH2 domain of Fyn to NS5A (Fig. 2B). Arg^{176} is located in the consensus sequence within the SH2 domains to interact with phosphotyrosine residue. On the other hand, the SH3 domain of these kinases associated with NS5A to a comparable level (Fig. 2C). These results suggest that

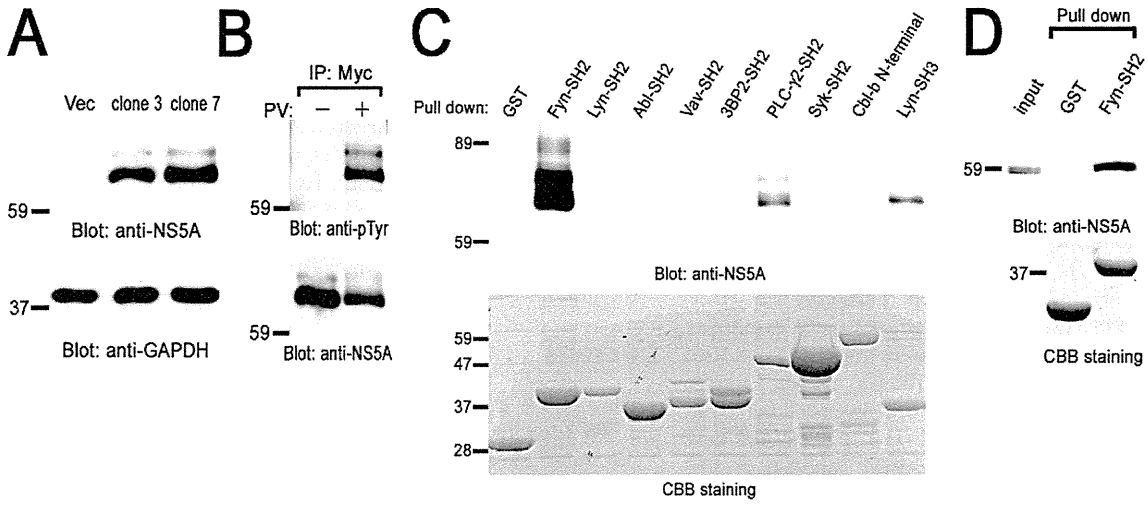

Figure 1. Identification of HCV NS5A-interacting proteins in B cells. (A) Generation of stable B cell lines expressing HCV NS5A. Detergent soluble cell lysates from vector cells (Vec) and Myc-His-NS5A expressing clones (clones 3 and 7) were separated by SDS-PAGE and analyzed with immunoblotting with anti-NS5A and anti-GAPDH mAbs. (B) BJAB cells expressing Myc-His-NS5A (clone 7) were treated without (−) or with (+) PV and solubilized in the lysis buffer. Cell lysates were immunoprecipitated with anti-Myc mAb and immunoprecipitated proteins were separated by SDS-PAGE and analyzed with immunoblotting with anti-pTyr (PY20) and anti-NS5A mAbs. PV-treated cells expressing Myc-His-NS5A (clone 7) (C) or Huh-7.5 cells stably harboring an HCV subgenomic replicon (D) were solubilized in the binding buffer. Precleared lysates were reacted with the indicated GST-fusion proteins and binding proteins were separated by SDS-PAGE and analyzed with immunoblotting with anti-NS5A mAb. The amount of GST-fusion proteins was confirmed by Coomassie brilliant blue (CBB) staining (C and D). Molecular sizing markers are indicated at left in kilodalton. The results were representative of three independent experiments. Similar results were obtained when another line was examined (B and C).
doi:10.1371/journal.pone.0046634.g001

increase in tyrosine phosphorylation of NS5A itself, or other associating proteins, allow the interaction with the SH2 domain of Fyn.

Central and/or C-terminal regions of NS5A binds to the SH2 domain of Fyn

To map the Fyn-SH2-binding region in NS5A, a series of deletion mutants were examined (Fig. 3). The results obtained reveals that N-terminal region (amino acids number 1–126) is not required for the interaction with the SH2 domain of Fyn in COS cells, although this region contains the region to interact with another kinase Syk (Fig. 3A) [11]. NS5A 127–146 and 147–447 could interact with the SH2 domain of Fyn. This demonstrates that deletion of the Fyn-binding region in the context of the full-length protein leads to loss of function. Similar results were obtained when HCV NS5A proteins were transiently expressed in Ramos B cells expressing SV40 T antigen (Ramos-T cells), and examined by pull-down assay (Fig. 3B). Deletion of 127–146 (NS5A Δ127–146) still allowed binding of NS5A to the SH2

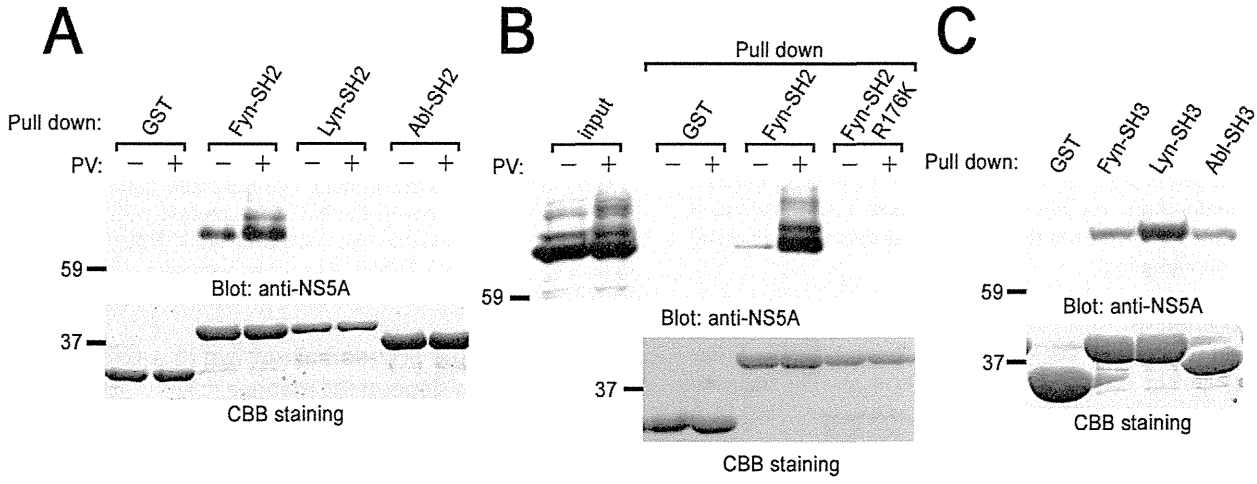

Figure 2. Pervanadate treatment of cells stimulates the binding of NS5A to the SH2 domain of Fyn in B cells. Either nontreated or PV-pretreated cells expressing Myc-His-NS5A (clone 7) were reacted with GST-fusion proteins of SH2 domains of various protein-tyrosine kinases (PTKs) (A), GST-Fyn-SH2 or GST-Fyn-SH2 R176K (B), or SH3 domains of various PTKs (C). Binding proteins were separated by SDS-PAGE and analyzed with immunoblotting with anti-NS5A mAb. The amount of GST-fusion proteins was confirmed by CBB staining. Molecular sizing markers are indicated at left in kilodalton. The results were representative of three independent experiments. Similar results were obtained when another line was examined.
doi:10.1371/journal.pone.0046634.g002

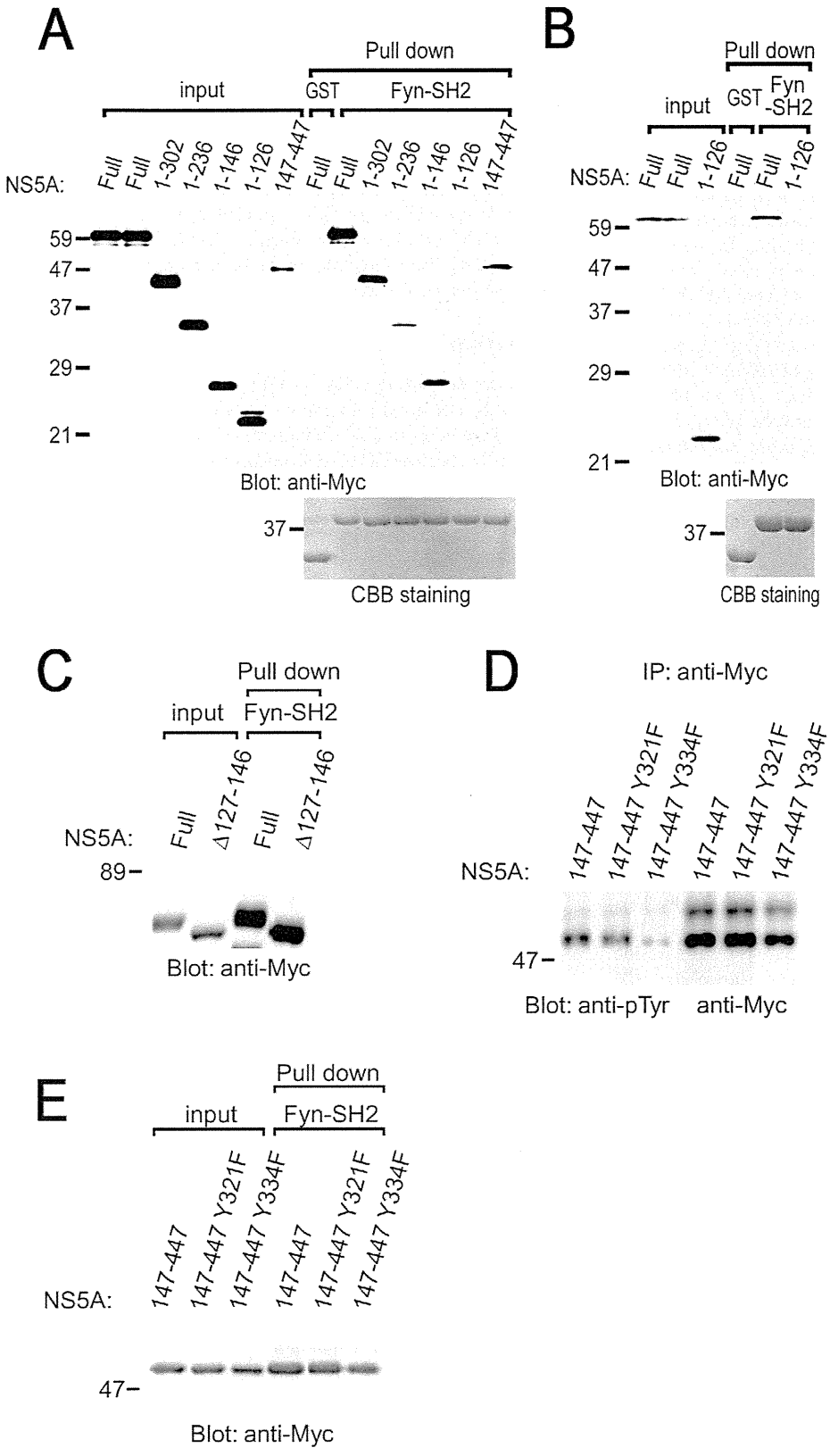

Figure 3. Structural analysis of the association of NS5A with the SH2 domain of Fyn in B cells. COS cells (A, C, E) or B cells (Ramos-T) (B) expressing different kinds of NS5A were stimulated with PV and subjected to pull-down assay using GST-Fyn-SH2. Binding proteins were separated by SDS-PAGE and analyzed with immunoblotting with anti-Myc mAb. The amount of GST-fusion proteins was confirmed by CBB staining. (D) COS cells expressing different kinds of NS5A mutants were stimulated with PV and subjected to immunoprecipitation. Precipitated proteins were separated by SDS-PAGE and analyzed with immunoblotting with anti-pTyr (PY20) and anti-Myc mAbs. Molecular sizing markers are indicated at left in kilodalton. The results were representative of three independent experiments.
doi:10.1371/journal.pone.0046634.g003

domain of Fyn (Fig. 3C). This suggests that NS5A Δ127–146 could interact with the SH2 domain of Fyn through NS5A 147–447.

Identification of Tyr^{334} as a tyrosine phosphorylation site in NS5A

In COS cells, full length and a series of deletion mutants of NS5A were tyrosine phosphorylated by PV treatment (Fig. S2). Because NS5A 1–126 could not bind to the SH2 domain of Fyn, we examined the possible involvement of tyrosine residue between amino acids number 127 and 146 for the binding. In this region, there is only one tyrosine residue that appears to be conserved. However, substitution of Tyr^{129} to Phe of truncated NS5A (NS5A 1–146 Y129F) still allowed tyrosine phosphorylation by PV and binding to the SH2 domain of Fyn in COS cells (Fig. S2 and S3). Thus, Tyr^{129} is not critical for the binding of NS5A to the SH2 domain of Fyn. In addition to this region (127 to 146), we examined the conserved tyrosine residues between 147 and 447 of NS5A (Tyr^{182}, Tyr^{321}, and Tyr^{334}). Among those, substitution of Tyr^{334} to Phe (Y334F) reduced tyrosine phosphorylation of NS5A 147–447, however this mutant could interact with the SH2 domain of Fyn (Fig. 3D and E). NS5A Y182F and Y321F were tyrosine phosphorylated as NS5A 147–447 (Fig. 3D and data now shown). Therefore, these results suggest that Tyr^{334} is required for tyrosine phosphorylation of NS5A, and existence of the multiple mechanisms for the binding of NS5A with Fyn including pTyr-SH2 domain interaction. Furthermore, we could not detect the increase in tyrosine phosphorylation of NS5A by *in vitro* kinase reaction with Fyn (data not shown), suggesting that some other protein-tyrosine kinases are required for phosphorylating NS5A.

The SH2 domain of Fyn directly binds to NS5A

Next we examined the mechanism of the interaction of the SH2 domain of Fyn and NS5A. Association of Fyn and NS5A in B cells were tested by the immunoprecipitation study (Fig. 4A). The result showed that NS5A was coprecipitated with anti-Fyn antibody, and vice versa. Therefore, NS5A complexes with Fyn in B cells. Far-western analysis further demonstrated that the SH2 domain of Fyn could directly bind to NS5A, suggesting that NS5A is tyrosine phosphorylated in B cells (Fig. 4B). We have shown that PV treatment of cells stimulates tyrosine phosphorylation of NS5A (Fig. 1B). These results demonstrate that NS5A could be tyrosine phosphorylated in B cells and directly associated with the SH2 domain of Fyn. In addition, we demonstrated the subcellular fractionation by sucrose density gradient centrifugation (Fig. 4C). Fractions 2–4 were regarded as low density detergent-insoluble fractions, whereas 5–9 were detergent-soluble fractions. As shown, NS5A broadly located in almost all of the fractions. In contrast, most of Fyn was located in detergent-insoluble fractions because of the lipid modification of Fyn (fractions 2–4), and some were in the detergent-soluble fractions (fractions 5–9). These results demonstrate that some of NS5A and Fyn are located in low density detergent-insoluble fractions in B cells.

Association with NS5A increases autophosphorylation and kinase activity of Fyn

Finally, we examined the effect of the expression of NS5A on the function of Fyn tyrosine kinase (Fig. 4D). Cross-linking of B cell receptor by anti-IgM mAb resulted in the increase in phosphorylation of a tyrosine residue in the activation loop of the kinase domain of Fyn, which parallels to its kinase activity [10]. Immunoprecipitation and immunoblotting experiments demonstrated that coexpression of NS5A increases phosphorylation of activation loop tyrosine and anti-IgM stimulation enhances this phenomenon. Immunoblot quantification also indicated the significant higher phosphorylation of the activation loop of Fyn in the unstimulated state in the NS5A expressing cells. In addition, we examined the biochemical kinase activity of Fyn by *in vitro* kinase assay (Fig. 4E). Coexpression of NS5A enhanced the kinase activity of Fyn as measured by both autophosphorylation and phosphorylation of exogenous substrate (enolase). This result biochemically demonstrated that association with NS5A increases tyrosine kinase activity of Fyn to phosphorylate tyrosine residues on Fyn itself and exogenous substrate. These results suggest that association of NS5A enhances an autophosphorylation and kinase activity of Fyn in B cells.

Discussion

We have demonstrated the possible tyrosine phosphorylation of NS5A in B cells and the interaction of NS5A with the SH2 domain of Fyn, in addition to SH3 domain. Previous reports demonstrated that cells harboring HCV replicon possesses the increased kinase activity of Fyn, which supports our conclusion of this study [9]. NS5A contains a highly conserved proline rich regions with Pro-X-X-Pro-X-Arg motif which is capable of the interaction with the SH3 domains of variety of cellular proteins, including Fyn [24]. Our finding reveals the second interaction site of Fyn to associate with NS5A. Therefore, NS5A could associate with both SH3 and SH2 domains. Through the two interactions, via SH3 and SH2 domains, it is predicted that NS5A could alter the conformation of Fyn to open active state. Physiological mechanism has generally been recognized that adaptor proteins with ligands of SH2 and SH3 domains bind to Src family kinases and positively regulates the kinase activity. Consistent with previous reports, our study demonstrated that NS5A protein containing potential ligands for both SH3 and SH2 domains increases autophosphorylation of Fyn in B cells.

Fyn has two tyrosine phosphorylation sites; one tyrosine in the activation loop is phosphorylated by autophosphorylation and the other in the C-terminal tail is phosphorylated by Csk to negatively regulate the kinase activity. In this manuscript, we examine the phosphorylation of tyrosine in the activation loop by using anti-phospho-Src family (Tyr416) antibody, which detects phosphorylated amount of a conserved tyrosine in the activation loop of Src family kinase (Fig. 4D). Therefore, we could conclude that tyrosine phosphorylation of Fyn was occurred in Tyr^{420} in the kinase domain.

The small interference RNA library screening study demonstrated that Csk is one of the protein-tyrosine kinases involved in the replication of HCV [25]. Csk is known to phosphorylate tyrosine residue in the C-terminal tail and negatively regulate Src family kinase, such as Fyn. Knock down of Fyn resulted in up-regulation of HCV replication [25]. This suggests that activation of Fyn suppresses HCV replication. In light of the aberrant increase in autophosphorylation of Fyn by NS5A coexpression, it is possible that NS5A negatively regulates HCV replication with activating Fyn kinase assumedly for persistent infection.

v-Src is the first discovered oncogene, and Fyn is a member of cellular Src family kinases and is also associated with cancer. Overexpression of Fyn in NIH3T3 fibroblast cells exhibited a cancer-like phonotype with increased anchorage-independent growth and prominent morphologic changes. Other studies have revealed that overexpression of Fyn results in promotion of the anti-apoptotic activity of Akt and dysregulation of anchorage-dependent cell growth. In this study, expression of NS5A enhanced autophosphorylation of Fyn in B cells, suggesting that

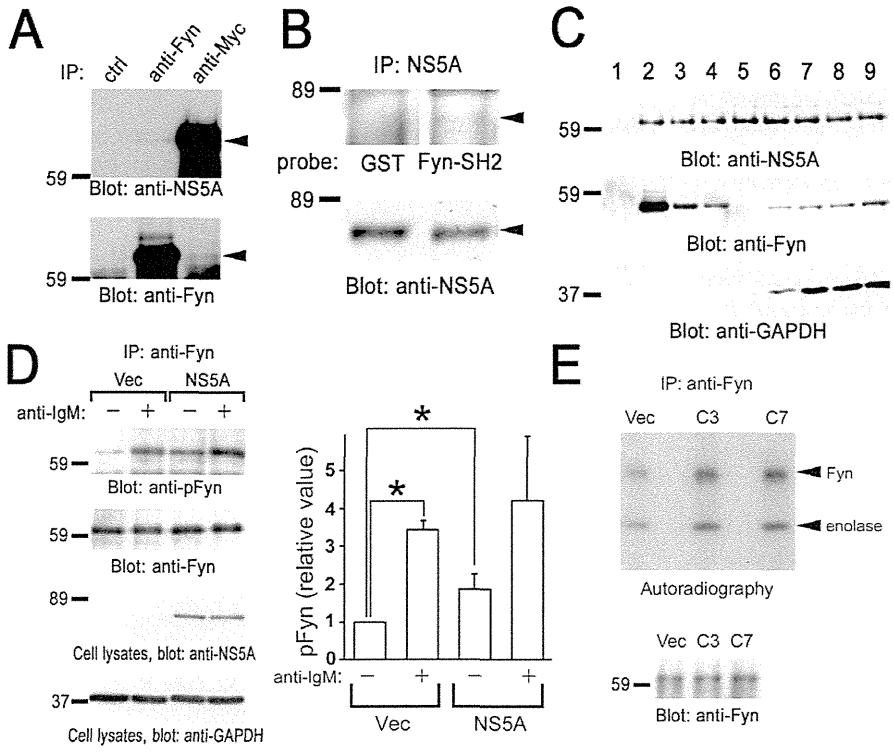

Figure 4. Association with NS5A increases the kinase activity of Fyn in B cells. (A) Endogenous interaction of Fyn with NS5A in BJAB cells. Cells were solubilized in the lysis buffer containing 0.5% Nonidet P-40. Detergent-soluble lysates from BJAB cells expressing Myc-His-NS5A (clone 7) were subjected to immunoprecipitation with anti-Fyn or anti-Myc antibodies. Protein interactions between NS5A and Fyn were analyzed by the immunoblotting with anti-NS5A mAb and anti-Fyn antibody, respectively. (B) Anti-Myc immunoprecipitates were separated by SDS-PAGE and subjected to far western analysis with GST or GST-Fyn-SH2 (GST-Fyn-SH2) (upper panel), and immunoblotting analysis with anti-NS5A mAb (lower panel). (C) Cell homogenates were fractionated by sucrose density gradient centrifugation. Proteins from these fractions were separated by SDS-PAGE and analyzed with immunoblotting with anti-NS5A mAb, anti-Fyn, and anti-GAPDH antibodies. (D) Control cells (Vec) and cells expressing Myc-His-NS5A (clone 7) were unstimulated (−) or stimulated (+) with anti-IgM mAb. Anti-Fyn immunoprecipitates (IP) were separated by SDS-PAGE and analyzed by immunoblotting with anti-phospho-Src family (Tyr416) antibody recognizing autophosphorylated Fyn (pFyn) and anti-Fyn antibody. Detergent-soluble lysates were separated by SDS-PAGE and analyzed by immunoblotting with anti-NS5A and anti-GAPDH mAbs. Densitometry analysis was performed on three experiments representative of Fig. 4D. Levels of pFyn were normalized to their respective total Fyn protein. The fold changes of pFyn are shown relative to unstimulated control cells. Data represent the mean ± SD of three independent experiments. *, $P<0.05$. (E) Anti-Fyn immunoprecipitates (IP) from control cells (Vec), cells expressing Myc-His-NS5A clone 3 (C3) and clone 7 (C7) were subjected to *in vitro* kinase assay using enolase as an exogenous substrate. Radioactive proteins were separated by SDS-PAGE and visualized by autoradiography. Immunoprecipitated Fyn was analyzed by immunoblotting. Molecular sizing markers are indicated at left in kilodalton. The results were representative of three independent experiments. Similar results were obtained when another line was examined.
doi:10.1371/journal.pone.0046634.g004

HCV-mediated activation of Fyn can promote aberrant growth and anti-apoptotic status leading to B lymphomagenesis [8].

Adaptor proteins have also been recognized candidates to promote oncogenes. For example, v-Crk (CT10 regulator of tyrosine kinase)/Crk-I are adaptor proteins composed of SH2 and SH3 domains but lack negative regulatory region (phosphotyrosine and C-terminal SH3 domain). Those adaptors function as constitutively activated ones, leading to tumorgenesis. Like that, NS5A presumably works constitutive activated adaptor for Fyn kinase [26].

In conclusion, present study demonstrated that NS5A binds to the SH2 domain of Fyn in tyrosine phosphorylation-dependent manner and that NS5A containing ligand for both SH2 and SH3 domains produces an aberrant increase in autophosphorylation and kinase activity of Fyn. Further studies are needed to clarify which tyrosine residues in NS5A are phosphorylated and bind to SH2 domain of Fyn. These data, however, may contribute to our understanding of the mechanisms that HCV infection causes B lymphomagenesis.

Supporting Information

Figure S1 GST-human Fyn-SH2 could react with NS5A. The cDNA for human Fyn-SH2 (Trp^{149}-Arg^{268}) were amplified by PCR using paired primers 5′-GGAATTCATGGTACTTTG-GAAAACTTGGC-3′ and 5′-GATCAACTGCAGGGATTCT-CG -3′, using cDNA from total RNA of BJAB cells as a template. Resulted PCR fragment was subcloned into the pGEX-4T.3 (GE Healthcare) to make domain in-frame with the downstream of GST and verified by DNA sequencing. PV-treated cells expressing Myc-His-NS5A (clone 7) were solubilized in the lysis buffer. Precleared lysates were reacted with GST or GST-human Fyn-SH2 and binding proteins were separated by SDS-PAGE and analyzed with immunoblotting with anti-NS5A mAb. The amount of GST-fusion proteins was confirmed by CBB staining. Molecular sizing markers are indicated at left in kilodalton. The results are representative of two independent experiments.
(TIF)

Figure S2 Tyrosine phosphorylation of NS5A and its mutants in COS cells. Full length and a series of deletion

mutants of NS5A were transiently expressed in COS cells. Cells were unstimulated (−) or stimulated (+) with PV and solubilized in the lysis buffer. Cell lysates were immunoprecipitated with anti-Myc mAb and immunoprecipitated proteins were separated by SDS-PAGE and analyzed with immunoblotting with anti-pTyr (PY20) and anti-Myc mAbs. Molecular sizing markers are indicated at left in kilodalton. The results were representative of three independent experiments.
(TIF)

Figure S3 Tyr^{129} is not critical for the binding of NS5A to the SH2 domain of Fyn. Indicated mutant forms of NS5A were transiently expressed in COS cells. Cells were unstimulated (−) or stimulated (+) with PV. Cells were solubilized in the binding buffer and precleared lysates were reacted with GST-Fyn-SH2. Detergent-soluble lysates and binding proteins were separated by SDS-PAGE and analyzed with immunoblotting with anti-Myc mAb. Molecular sizing markers are indicated at left in kilodalton. The results were representative of three independent experiments.
(TIF)

Acknowledgments

We are grateful to Dr. R. Bartenschlager (University of Heidelberg, Germany) for providing an HCV subgenomic replicon (pFK5B/2884 Gly), to Ms. Satomi Nishibata and Ms. Kuniyo Miyagoshi for the assistance, and to Dr. Shinkou Kyo (Kobe University Graduate School of Medicine, Toyooka Public Hospital, Hyogo, Japan) and Dr. Keiko Kawauchi (Mechanobiology Institute, Singapore) for experimental assistance.

Author Contributions

Conceived and designed the experiments: KN KT HH KS. Performed the experiments: KN KT TH XS KS. Analyzed the data: KN KT KC HH KS. Contributed reagents/materials/analysis tools: KN KT KC TH XS LD IS HH KS. Wrote the paper: KN HH KS.

References

1. Moradpour D, Penin F, Rice CM (2007) Replication of hepatitis C virus. Nat Rev Microbiol 5: 453–463.
2. Suzuki T, Aizaki H, Murakami K, Shoji I, Wakita T (2007) Molecular biology of hepatitis C virus. J Gastroenterol 42: 411–423.
3. Agnello V, Chung RT, Kaplan LM (1992) A role for hepatitis C virus infection in type II cryoglobulinemia. New Engl J Med 327: 1490–1495.
4. Morsica G, Tambussi G, Sitia G, Novati R, Lazzarin A, et al. (1999) Replication of hepatitis C virus in B lymphocytes (CD19(+)). Blood 94: 1138–1139.
5. Gisbert JP, Garcia-Buey L, Pajares JM, Moreno-Otero R (2003) Prevalence of hepatitis C virus infection in B-cell non-Hodgkin's lymphoma: Systematic review and meta-analysis. Gastroenterology 125: 1723–1732.
6. Machida K, Cheng KTH, Pavio N, Sung VMH, Lai MMC (2005) Hepatitis C virus E2-CD81 interaction induces hypermutation of the immunoglobulin gene in B cells. J Virol 79: 8079–8089.
7. Ito M, Murakami K, Suzuki T, Mochida K, Suzuki M, et al. (2010) Enhanced expression of lymphomagenesis-related genes in peripheral blood B cells of chronic hepatitis C patients. Clin Immunol 135: 459–465.
8. Saito YD, Jensen AR, Salgia R, Posadas EM (2010) Fyn A Novel Molecular Target in Cancer. Cancer 116: 1629–1637.
9. Macdonald A, Crowder K, Street A, McCormick C, Harris M (2004) The hepatitis C virus NS5A protein binds to members of the Src family of tyrosine kinases and regulates kinase activity. J Gen Virol 85: 721–729.
10. Bradshaw JM (2010) The Src, Syk, and Tec family kinases: Distinct types of molecular switches. Cell Signal 22: 1175–1184.
11. Inubushi S, Nagano-Fujii M, Kitayama K, Tanaka M, An C, et al. (2008) Hepatitis C virus NS5A protein interacts with and negatively regulates the non-receptor protein tyrosine kinase Syk. J Gen Virol 89: 1231–1242.
12. Pfannkuche A, Buther K, Karthe J, Poenisch M, Bartenschlager R, et al. (2011) c-Src is required for complex formation between the hepatitis C virus-encoded proteins NS5A and NS5B: A prerequisite for replication. Hepatology 53: 1127–1136.
13. Ishido S, Choi JK, Lee BS, Wang CY, DeMaria M, et al. (2000) Inhibition of natural killer cell-mediated cytotoxicity by kaposi's sarcoma-associated herpesvirus K5 protein. Immunity 13: 365–374.
14. Ogi K, Nakashima K, Chihara K, Takeuchi K, Horiguchi T, et al. (2011) Enhancement of B-cell receptor signaling by a point mutation of adaptor protein 3BP2 identified in human inherited disease cherubism. Genes Cells 16: 951–960.
15. Sada K, Miah SM, Maeno K, Kyo S, Qu X, et al. (2002) Regulation of FcεRI-mediated degranulation by an adaptor protein 3BP2 in rat basophilic leukemia RBL-2H3 cells. Blood 100: 2138–2144.
16. Rao N, Ghosh AK, Ota S, Zhou P, Reddi AL, et al. (2001) The non-receptor tyrosine kinase Syk is a target of Cbl-mediated ubiquitylation upon B-cell receptor stimulation. EMBO J 20: 7085–7095.
17. Shukla U, Hatani T, Nakashima K, Ogi K, Sada K (2009) Tyrosine Phosphorylation of 3BP2 Regulates B Cell Receptor-mediated Activation of NFAT. J Biol Chem 284: 33719–33728.
18. Blight KJ, McKeating JA, Rice CM (2002) Highly permissive cell lines for subgenomic and genomic hepatitis C virus RNA replication. J Virol 76: 13001–13014.
19. Nakashima K, Takeuchi K, Chihara K, Hotta H, Sada K (2011) Inhibition of hepatitis C virus replication through adenosine monophosphate-activated protein kinase-dependent and -independent pathways. Microbiol Immunol 55: 774–782.
20. Maeno K, Sada K, Kyo S, Miah SM, Kawauchi-Kamata K, et al. (2003) Adaptor protein 3BP2 is a potential ligand of Src homology 2 and 3 domains of Lyn protein-tyrosine kinase. J Biol Chem 278: 24912–24920.
21. Miah SM, Hatani T, Qu X, Yamamura H, Sada K (2004) Point mutations of 3BP2 identified in human inherited disease cherubism results in the loss of function. Genes Cells 9: 993–1004.
22. Chihara K, Nakashima K, Takeuchi K, Sada K (2011) Association of 3BP2 with SHP-1 regulates SHP-1-mediated production of TNF-α in RBL-2H3 cells. Genes Cells 16: 1133–1145.
23. Qu X, Sada K, Kyo S, Maeno K, Miah SM, et al. (2004) Negative regulation of FcεRI-mediated mast cell activation by a ubiquitin-protein ligase Cbl-b. Blood 103: 1779–1786.
24. Shelton H, Harris M (2008) Hepatitis C virus NS5A protein binds the SH3 domain of the Fyn tyrosine kinase with high affinity: mutagenic analysis of residues within the SH3 domain that contribute to the interaction. Virol J 5: 24. Available: http://www.virologyj.com/content/5/1/24.
25. Supekova L, Supek F, Lee J, Chen S, Gray N, et al. (2008) Identification of human kinases involved in hepatitis C virus replication by small interference RNA library screening. J Biol Chem 283: 29–36.
26. Birge RB, Kalodimos C, Inagaki F, Tanaka S (2009) Crk and CrkL adaptor proteins: networks for physiological and pathological signaling. Cell Commun Signal 7: 13. Available: http://www.biosignaling.com/content/7/1/13.

Polymorphisms of the Core, NS3, and NS5a Proteins of Hepatitis C Virus Genotype 1b Associate with Development of Hepatocellular Carcinoma

Ahmed El-Shamy,[1,2]* Michiko Shindo,[3]* Ikuo Shoji,[1] Lin Deng,[1] Tadao Okuno,[3] and Hak Hotta[1]

Hepatocellular carcinoma (HCC) is one of the common sequels of hepatitis C virus (HCV) infection. It remains controversial, however, whether HCV itself plays a direct role in the development of HCC. Although HCV core, NS3, and NS5A proteins were reported to display tumorigenic activities in cell culture and experimental animal systems, their clinical impact on HCC development in humans is still unclear. In this study we investigated sequence polymorphisms in the core protein, NS3, and NS5A of HCV genotype 1b (HCV-1b) in 49 patients who later developed HCC during a follow-up of an average of 6.5 years and in 100 patients who did not develop HCC after a 15-year follow-up. Sequence analysis revealed that Gln at position 70 of the core protein (core-Gln^{70}), Tyr at position 1082 plus Gln at 1112 of NS3 (NS3-Tyr^{1082}/Gln^{1112}), and six or more mutations in the interferon/ribavirin resistance-determining region of NS5A (NS5A-IRRDR≥6) were significantly associated with development of HCC. Multivariate analysis identified core-Gln^{70}, NS3-Tyr^{1082}/Gln^{1112}, and α-fetoprotein (AFP) levels (>20 ng/L) as independent factors associated with HCC. Kaplan-Meier analysis revealed a higher cumulative incidence of HCC for patients infected with HCV isolates with core-Gln^{70}, NS3-Tyr^{1082}/Gln^{1112} or both than for those with non-(Gln^{70} plus NS3-Tyr^{1082}/Gln^{1112}). In most cases, neither the residues at position 70 of the core protein nor positions 1082 and 1112 of the NS3 protein changed during the observation period. *Conclusion*: The present results suggest that HCV isolates with core-Gln^{70} and/or NS3-Tyr^{1082}/Gln^{1112} are more closely associated with HCC development compared to those with non-(Gln^{70} plus NS3-Tyr^{1082}/Gln^{1112}). (HEPATOLOGY 2012;00:000–000)

Hepatitis C virus (HCV) is a major etiologic agent of chronic hepatitis worldwide, with the estimated number of infected individuals being more than 180 million. Approximately 15% to 20% of chronically infected individuals undergo liver cirrhosis in a decade or so after infection, with hepatocellular carcinoma (HCC) arising from cirrhosis at an estimated rate of 1% to 4% per year.[1-3] Several host factors such as male gender, older age, elevated α-fetoprotein (AFP) level, advanced liver fibrosis as well as nonresponsiveness to interferon (IFN) therapy have been reported as important predictors of HCC development.[4,5] Recently, a host genetic factor, i.e., the *DEPDC5* locus polymorphism, was reported to be associated with progression to HCC in HCV-infected individuals.[6] On the other hand, it remains controversial as to whether HCV itself plays a direct role in the development of HCC. Experimental data suggest that HCV contributes to HCC by modulating pathways that promote malignant transformation of hepatocytes. HCV core, NS3, and NS5A proteins were shown to be involved in a number of potentially oncogenic pathways in cell culture and experimental animal systems.[7] HCV core protein rendered cultured cells more resistant to apoptosis[8,9] and promoted *ras* oncogene-mediated transformation.[10,11]

Abbreviations: HCC, hepatocellular carcinoma; HCV, hepatitis C virus; IFN, interferon; IRRDR, interferon/ribavirin resistance-determining region; ISDR, interferon sensitivity-determining region.

From the [1]Division of Microbiology, Kobe University Graduate School of Medicine, Kobe, Japan; [2]Department of Virology, Suez Canal University Faculty of Veterinary Medicine, Ismalia, Egypt; and [3]Department of Gastroenterology, Akashi City Hospital, Akashi, Japan.

Received September 3, 2012; accepted December 9, 2012.

Supported in part by Health and Labour Sciences Research Grants from the Ministry of Health, Labour and Welfare, Japan, and a SATREPS Grant from Japan Science and Technology Agency (JST) and Japan International Cooperation Agency (JICA). This study was also carried out as part of Japan Initiative for Global Research Network on Infectious Diseases (J-GRID), Ministry of Education, Culture, Sports, Science and Technology, Japan, and the Global Center of Excellence (G-COE) Program at Kobe University Graduate School of Medicine.

*These authors contributed equally to this work.

Current address for Ahmed El-Shamy: Division of Liver Diseases, Mount Sinai School of Medicine, New York, New York, USA..

Moreover, transgenic mice expressing the HCV core protein in the liver developed HCC.[12] However, the clinical impact of HCV proteins on HCC development in humans and whether all HCV isolates are equally associated with HCC is yet to be determined. In a clinical setting, HCV core protein mutations at positions 70 (Gln^{70}) and/or 91 (Met^{91}) were closely associated with HCC development.[13-16] Gln^{70} and/or Met^{91} were also linked to resistance to PEG-IFN/ribavirin (RBV) treatment.[17-20] In addition, we and other investigators reported that an N-terminal part of the NS3 protein has the capacity to transform NIH3T3 and rat fibroblast cells[21,22] and to render NIH3T3 cells more resistant to DNA damage-induced apoptosis, which is thought to be a prerequisite for malignant transformation of the cell.[23] Also, the NS5A protein is a pleiotropic protein with key roles in both viral RNA replication and modulation of the host cell functions.[24] In particular, the links between NS5A and the IFN responses have been widely discussed. It was proposed initially that sequence variations within a region in NS5A spanning from amino acids (aa) 2209 to 2248, called the IFN sensitivity-determining region (ISDR), were correlated with IFN responsiveness.[25] Subsequently, in the era of PEG-IFN/RBV combination therapy, we identified a new region near the C-terminus of NS5A spanning from aa 2334 to 2379, which we referred to as the IFN/RBV resistance-determining region (IRRDR).[26,27] The degree of sequence variations within the IRRDR was significantly associated with the clinical outcome of PEG-IFN/RBV therapy. In the context of HCC, several retrospective studies suggested that IFN-based therapy might reduce the risk of HCC development.[4,28-30]

In an attempt to clarify whether viral factors, in particular those within the core, NS3, and NS5A proteins, are involved in HCC development, we carried out a comparative analysis of the aa sequences obtained from HCV patients who developed HCC and those who did not. In addition, we studied the sequence evolution of these genes in the interval between chronic hepatitis C and HCC development over a period of 15 years.

Patients and Methods

Ethics Statement. The study protocol, which conforms to the provisions of the 1975 Declaration of Helsinki, was approved beforehand by the Ethic Committees in Akashi City Hospital and Kobe University Graduate School of Medicine, and written informed consent was obtained from each patient enrolled in this study.

Patients. A total of 49 HCV-infected patients who developed HCC (HCC group) were retrospectively examined. They were followed up (from 1988 to 2003) with an average period until HCC development being 6.5 ± 2.9 years. Paired serum samples at the time of chronic hepatitis C (pre-HCC sample) and HCC development (post-HCC sample) were collected. As a control group, 100 HCV-infected patients who were followed up over a period of 15 years (from 1988 to 2003) without HCC development were retrospectively examined. Serum samples of the control group were available at the time of first visit to the clinic. All patients enrolled in this study were chronically infected with HCV genotype 1b (HCV-1b). HCV subtype was determined as reported previously.[31] Serum HCV RNA titers were quantitated by reverse-transcription polymerase chain reaction (RT-PCR0 with an internal RNA standard derived from the 5′ noncoding region of HCV (Amplicor HCV Monitor test, v. 2.0, Roche Diagnostics, Tokyo, Japan). All patients underwent liver biopsy and were diagnosed as chronic hepatitis. All HCC and 68% (68/100) of non-HCC patients received IFN-monotherapy, either natural IFN alpha (Sumiferon, Dainipponsumitomo Pharmaceutical, Osaka, Japan) at a dose of 6 million units (MU) or recombinant IFN alpha 2b (Intron A; Schering-Plough, Osaka, Japan) at a dose of 10 MU, 3 times a week for 6 months. All HCC patients were nonresponders (NR), who had detectable viremia during the entire course of IFN treatment. On the other hand, 18 (26%) of the 68 non-HCC patients treated with IFN achieved HCV RNA negativity at the end of treatment followed by rebound viremia within 6 months after the treatment and, therefore, they were referred to as relapsers. The other 50 IFN-treated, non-HCC patients were NR. The remaining 32 non-HCC patients did not receive IFN. All patients were seen every 2 months and tested for liver function markers during the follow-up period.

Sequence Analysis of HCV Core, NS3, and NS5A Proteins. HCV RNA was extracted from 140 μL of serum using a commercially available kit (QIAmp viral

Address reprint requests to: Hak Hotta, M.D., Ph.D., Division of Microbiology, Kobe University Graduate School of Medicine, 7-5-1 Kusunoki-cho, Chuo-ku, Kobe 650-0017, Japan. E-mail: hotta@kobe-u.ac.jp; fax: +81-78-382-5519.

Copyright © 2012 by the American Association for the Study of Liver Diseases.

View this article online at wileyonlinelibrary.com.

DOI 10.1002/hep.26205

Potential conflict of interest: Nothing to report.

RNA kit; Qiagen, Tokyo, Japan). The core, NS3, and NS5A regions of the HCV genome were amplified as described elsewhere.[26,32-34] The sequences of the amplified fragments were determined by direct sequencing. The aa sequences were deduced and aligned using GENETYX Win software version 7.0 (GENETYX, Tokyo, Japan). The numbering of aa was according to the polyprotein of the prototype of HCV-1b; HCV-J.[35]

Statistical Analysis. Statistical differences in the baseline parameters of HCC and control groups were determined by Student's t test for numerical variables and Fisher's exact probability or chi-square tests for categorical variables. Likewise, statistical differences in viral mutations between HCC and control groups were determined by Fisher's exact probability test. Kaplan-Meier analysis was performed to estimate the cumulative incidence of HCC. The data obtained were evaluated by the log-rank test. Univariate and multivariate logistic analyses were performed to identify variables that independently associated with HCC development. Variables with $P < 0.1$ in univariate analysis were included in a backward stepwise multivariate logistic regression analysis. The odds ratios and 95% confidence intervals (95% CI) were calculated. All statistical analyses were performed using SPSS v. 16 software (Chicago, IL). Unless otherwise stated, $P < 0.05$ was considered statistically significant.

Nucleotide Sequence Accession Numbers. The sequence data reported in this article have been deposited in the DDBJ/EMBL/GenBank nucleotide sequence databases with the accession numbers AB719460 through AB719842.

Results

Demographic Characteristics of HCC and Control Groups. The clinical characteristics of HCC and control groups are shown in Table 1. The HCC group had significantly higher titers of ALT, AST, and AFP, and higher fibrosis staging score than that of the control group. There was no significant difference in viremia titers between the two groups.

Table 1. Demographic Characteristics of HCC and Control Groups

Factor	HCC	Control	P-value
Age	57.3 ± 7.0*	56.4 ± 8.3	0.54
Sex (male/female)	31/18	54/46	0.29
ALT (IU/L)	159.4 ± 79.8	129.7 ± 51.5	0.007
AST (IU/L)	113.0 ± 62.2	91.6 ± 44.1	0.017
AFP (ng/L)	29.1 ± 33.7	18.4 ± 4.4	0.002
Platelets (x 10^4/mm^3)	16.2 ± 2.8	16.2 ± 2.4	0.88
Inflammation grading score	8.7 ± 0.9	8.4 ± 1.2	0.05
Fibrosis staging score	2.4 ± 0.5	2.2 ± 0.5	0.02
HCV-RNA (KIU/mL)	593.4 ± 112.3	618.1 ± 95.9	0.17

*Mean ± SD. HCC, hepatocellular carcinoma; ALT, alanine aminotransferase; AST, aspartate transaminase; AFP; α-fetoprotein.

Correlation Between Core Protein Sequence Polymorphism and HCC Development. HCV core protein sequences were obtained from all (49/49) and 94% (94/100) of pre-HCC and control patients' sera, respectively. Comparative sequence analysis revealed that 22 (45%) of 49 HCV isolates in the pre-HCC sera (pre-HCC isolates) and 59 (63%) of 94 HCV isolates from the control group (control isolates) had wild-core (Arg^{70}/Leu^{91}) (Table 2). The difference between HCC and control groups was hovering at a statistically significant level ($P = 0.05$). When the sequence pattern at position 70 alone was examined, a stronger association with HCC was observed. We found that 21 (43%) of 49 pre-HCC isolates had Gln^{70} while only 13 (14%) of 94 control isolates did ($P = 0.0002$). On the other hand, there was no significant correlation between sequence pattern at position 91 and HCC. Thus, a single mutation at position 70 (Gln^{70}) was the only polymorphic factor within core protein that was significantly associated with HCC development. It should be noted that there was no significant correlation between Gln^{70} and the degree of fibrosis progression (data not shown).

Correlation Between NS3 Protein Sequence Polymorphism and HCC Development. Sequences of NS3 serine protease domain (aa 1027 to 1146) were obtained from 94% (46/49) and 93% (93/100) of pre-HCC and control isolates, respectively. We found that 29 (63%) of 46 pre-HCC isolates had Tyr and Gln at positions 1082 and 1112, respectively (Tyr^{1082}/Gln^{1112}), while 39 (42%) of 93 control isolates did (Table 2). The difference in the proportion between pre-HCC and control isolates was statistically significant ($P = 0.029$). On the other hand, there was no significant correlation between Tyr^{1082}/Gln^{1112} and the degree of fibrosis progression (data not shown).

Correlation Between NS5A Protein Sequence Polymorphism and HCC Development. NS5A protein sequences were obtained from 92% (45/49) and 74% (74/100) of pre-HCC and control isolates, respectively. Twenty-four (53%) of 45 pre-HCC isolates had IRRDR of 6 or more mutations (IRRDR≥6) while only 15 (20%) of 74 control isolates did (Table 2; $P = 0.0003$). We also found that pre-HCC isolates tended to have a higher degree of sequence heterogeneity in ISDR than control isolates, although not statistically significant due probably to the small number of

Table 2. Correlation Between HCC and Sequence Polymorphic Factors of Core, NS3 and NS5A

HCV Protein	Factor	No. of Subjects / No. of Total* HCC	Control	P-value
Core	Wild-core (Arg^{70}/Leu^{91})	22/49 (45%)	59/94 (63%)	0.05
	Non-wild-core	27/49 (55%)	35/94 (37%)	
	Gln^{70}	21/49 (43%)	13/94 (14%)	0.0002
	Non-Gln^{70}	28/49 (57%)	81/94 (86%)	
	Leu^{91}	37/49 (76%)	70/94 (74%)	1.0
	Non- Leu^{91}	12/49 (24%)	24/94 (26%)	
NS3	Tyr^{1082} / Gln^{1112}	29/46 (63%)	39/93 (42%)	0.029
	Non-(Tyr^{1082} / Gln^{1212})	17/46 (37%)	54/93 (58%)	
NS5A	IRRDR≥6	24/45 (53%)	15/74 (20%)	0.0003
	IRRDR≤5	21/45 (47%)	59/74 (80%)	
	ISDR≥3	11/45 (24%)	8/74 (11%)	0.07
	ISDR≤2	34/45 (76%)	66/74 (89%)	
	Asn^{2218}	11/45 (24%)	3/74 (4%)	0.002
	Non-Asn^{2218}	34/45 (76%)	71/74 (96%)	

*Number of subjects with a given factor / total number of HCC or control. HCC, hepatocellular carcinoma; Arg^{70}, arginine at position 70 of the core protein; Leu^{91}, leucine at position 91 of the core protein; Gln^{70}, glutamine at position 70 of the core protein; Tyr^{1082}, tyrosine at position 1082 of NS3; Gln^{1212}, glutamine at position 1212 of NS3; IRRDR, interferon/ribavirin resistance-determining region; ISDR, interferon sensitivity-determining region; Asn^{2218}, asparagine at position 2218 of NS5A-ISDR.

cases examined; 11 (24%) of 45 pre-HCC isolates and 8 (11%) of 74 of control isolates had ISDR with three or more mutations ($P = 0.07$). Moreover, Asn at position 2218 (Asn^{2218}) within the ISDR was found in 24% (11/45) of pre-HCC isolates and only in 4% (3/74) of the control isolates ($P = 0.002$), suggesting that Asn^{2218} is significantly associated with development of HCC.

Cumulative HCC Incidence on the Basis of Core-Gln^{70}, NS3-Tyr^{1082}/Gln^{1112}, NS5A-IRRDR≥6, and NS5A-Asn^{2218}. Follow-up study revealed that the cumulative HCC incidence in patients infected with HCV-1b isolates with core protein of Gln^{70} and those of non-Gln^{70}, respectively, was 29% and 5% at the end of 5 years, 56% and 23% at the end of 10 years, and 63% and 26% at the end of 15 years (Fig. 1A), with the differences between the two groups being statistically significant ($P < 0.0001$; Log-rank test). Likewise, the cumulative HCC incidence in patients infected with HCV-1b isolates with NS3 of Tyr^{1082}/Gln^{1112} and those of non-(Tyr^{1082}/Gln^{1112}), respectively, was 15% and 7% at the end of 5 years, 37% and 24% at the end of 10 years, and 45% and 24% at the end of 15 years ($P = 0.02$) (Fig. 1B). Also, the cumulative HCC incidence in patients infected with HCV-1b isolates of IRRDR≥6 and those of IRRDR≤5, respectively, was 18% and 10% at the end of 5 years, 59% and 22% at the end of 10 years, and 63% and 27% at the end of 15 years ($P = 0.0002$) (Fig. 1C). Similarly, the cumulative HCC incidence in patients infected with HCV-1b isolates of Asn^{2218} and those of non-Asn^{2218}, respectively, was 31% and 9% at the end of 5 years, 77% and 28% at the end of 10 years, and 77% and 33% at the end of 15 years ($P = 0.0003$) (Fig. 1D).

Identification of Independent Factors Correlated with HCC Development by Univariate and Multivariate Logistic Regression Analyses. In order to identify significant independent factors associated with HCC development, all available data of baseline patients' parameters and core, NS3, and NS5A polymorphic factors were first analyzed by univariate logistic analysis. This analysis yielded eight factors that were significantly associated with HCC development: core-Gln^{70}, NS3-(Tyr^{1082}/Gln^{1112}), NS5A-IRRDR≥6, NS5A-Asn^{2218}, increased levels of ALT (>165 IU/L), AST (>65 IU/L), and AFP (>20 ng/L), and fibrosis staging score (≥3). Subsequently, those eight factors were entered in multivariate logistic regression analysis. This analysis identified two viral factors, core-Gln^{70} and NS3-(Tyr^{1082}/Gln^{1112}), and a host factor, AFP levels (>20 ng/L), as independent factors associated with HCC development (Table 3).

The vast majority of pre-HCC isolates (85%; 39/46) had core-Gln^{70} and/or NS3-Tyr^{1082}/Gln^{1112} and only 15% (7/46) had non-(Gln^{70} plus NS3-Tyr^{1082}/Gln^{1112}). By contrast, about a half of control isolates (52%; 46/89) had non-(Gln^{70} plus NS3-Tyr^{1082}/Gln^{1112}) (Fig. 2A). The difference in the proportion between HCC and control groups was statistically significant ($P < 0.0001$). Furthermore, the cumulative HCC incidence after 15-year follow-up was highest (63%) among patients with core-Gln^{70} plus NS3-(Tyr^{1082}/Gln^{1112}), whereas it was lowest (11%) among patients with non-(Gln^{70} plus NS3-Tyr^{1082}/Gln^{1112}) (Fig. 2B), with the difference being statistically significant ($P < 0.0001$; Log-rank test).

Evolution of the Sequences of the Core, NS3, and NS5A Proteins During the Follow-up Period from Chronic Hepatitis to HCC Development. Finally, we investigated sequence evolution of the core protein, NS3 and NS5A (IRRDR and ISDR) during the follow-up period from chronic hepatitis to HCC development by comparing the sequences between pre- and post-HCC isolates. The residue at position 70 of the core protein was conserved in 91% (41/45) of sequence pairs analyzed. The substitutions observed at this position were from Arg^{70} and His^{70} each to Gln^{70} in two cases and from Gln^{70} to Arg^{70} in the other two cases. The residues at positions 1082 and 1112 of

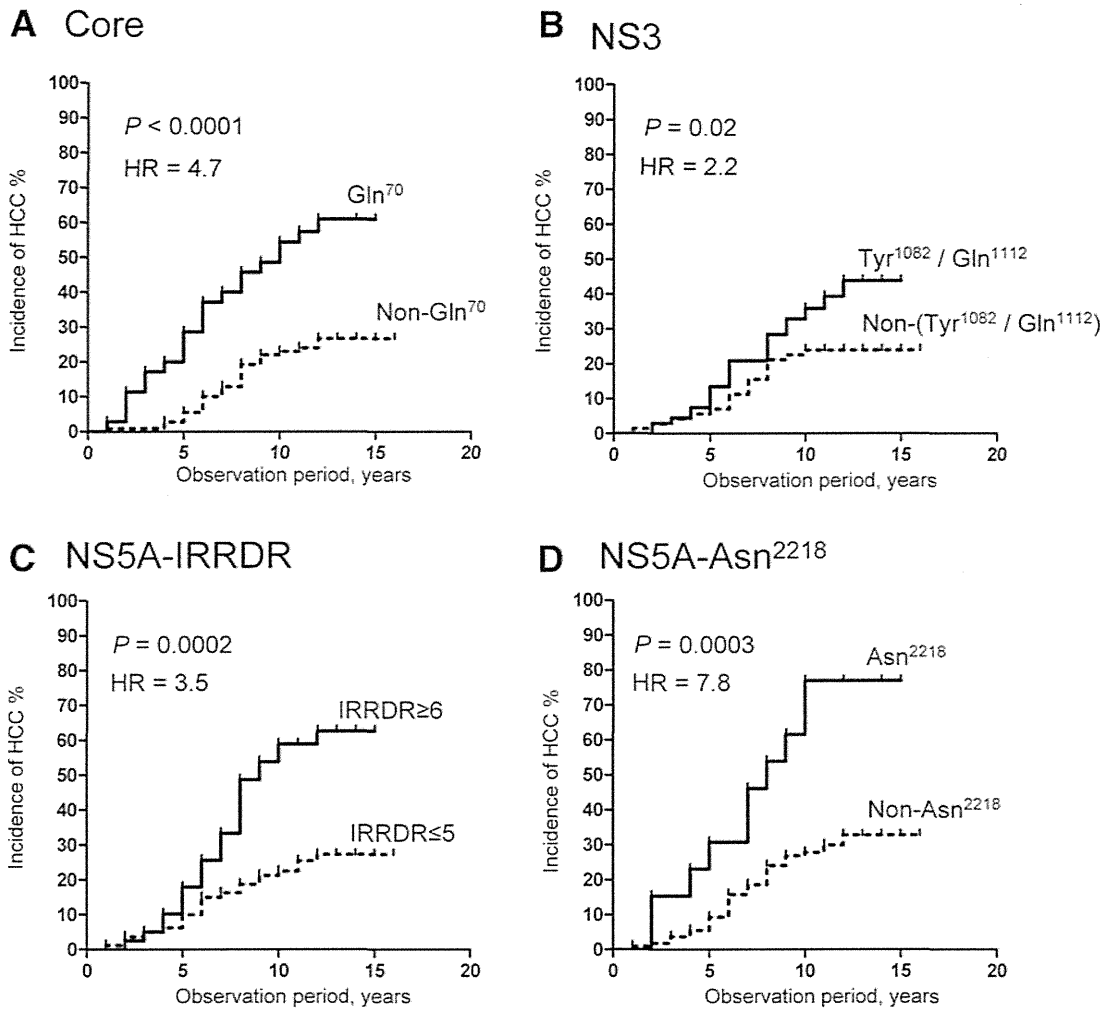

Fig. 1. Cumulative HCC incidence on the basis of HCV-1b sequence patterns. (A) Position 70 of the core protein. The numbers of core-Gln^{70} and non-Gln^{70} analyzed were 34 and 109, respectively. (B) Positions 1082 and 1112 of NS3. The numbers of NS3-(Tyr^{1082}/Gln^{1112}) and non-(Tyr^{1082}/Gln^{1112}) analyzed were 68 and 71, respectively. (C) NS5A-IRRDR. The numbers of NS5A-IRRDR≥6 and IRRDR≤5 analyzed were 39 and 80, respectively. (D) NS5A-Asn^{2218}. The numbers of NS5A-Asn^{2218} and non-Asn^{2218} analyzed were 14 and 105, respectively.

NS3 were conserved in 95% (41/43) and 100% (43/43), respectively, of the sequence pairs analyzed.

IRRDR and ISDR showed a high degree of sequence evolution. IRRDR sequences were different between pre- and post-HCC isolates in 66% (25/38) of cases analyzed (Fig. 3). IRRDR sequences tended to be more polymorphic at the time of HCC occurrence. Frequency of HCV isolates with IRRDR≥6 was F3

Table 3. Univariate and Multivariate Regression Analyses to Identify Independent Factors Associated with HCC

	Univariate		Multivariate	
Variable	Odds Ratio (95% CI)	*P*-value	Odds Ratio (95% CI)	*P*-value
Core-Gln^{70}	0.23 (0.10 - 0.52)	0.0004	6.8 (2.1 - 23.0)	0.001
NS3-Tyr^{1082} / Gln^{1212}	2.4 (1.1 - 4.9)	0.029	3.4 (1.1 - 10.0)	0.03
NS5A-IRRDR≥6	4.5 (2.0 - 10.0)	0.0003		
NS5A-Asn^{2218}	7.7 (2.0 - 29.0)	0.002		
AFP (>20 ng/L)	12 (5.1 - 30.0)	0.0001	19.5 (4.7 - 80.0)	0.0001
ALT (>165 IU/L)	4.0 (1.8 - 8.6)	0.0006		
AST (>65 IU/L)	3.9 (1.5 - 10.0)	0.003		
Fibrosis staging score (≥3)	2.4 (1.1 - 4.9)	0.02		

Gln^{70}, glutamine at position 70 of the core protein; Tyr^{1082}, tyrosine at position 1082 of NS3; Gln^{1212}, glutamine at position 1212 of NS3; IRRDR, interferon/ribavirin resistance-determining region; Asn^{2218}, asparagine at position 2218 of NS5A-ISDR, ALT, alanine aminotransferase; AST, aspartate transaminase; AFP; α-fetoprotein; IFN; interferon.

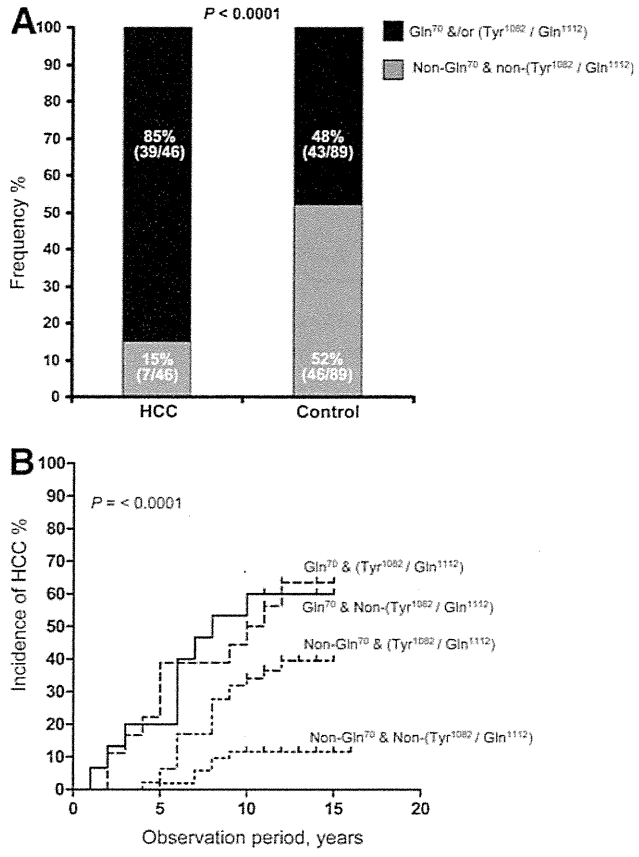

Fig. 2. (A) Proportions of HCV-1b isolates of the HCC high-risk group (core-Gln^{70} and/or NS3-[Tyr^{1082}/Gln^{1112}]) and the low-risk group (non-Gln^{70} and non-[Tyr^{1082}/Gln^{1112}]) among HCC and control groups. (B) Cumulative HCC incidence on the basis of different combined sequence patterns of position 70 of the core protein and positions 1082 and 1112 of NS3. Core-Gln^{70} and NS3-(Tyr^{1082}/Gln^{1112}), n = 18; core-Gln^{70} and non-(Tyr^{1082}/Gln^{1112}), n = 16; non-Gln^{70} and NS3-(Tyr^{1082}/Gln^{1112}), n = 48; non-Gln^{70}/non-(Tyr^{1082}/Gln^{1112}), n = 53.

significantly higher in post-HCC isolates than in pre-HCC isolates; IRRDR≥6 was found in 47% (18/38) of post-HCC isolates compared to 24% (9/38) of pre-HCC isolates ($P = 0.03$). On the other hand, ISDR≥3 was found in 21% (8/38) of post-HCC isolates compared to 11% (4/38) of pre-HCC isolates, with the difference between the two groups being not statistically significant ($P = 0.3$).

Discussion

HCC is one of the common long-term complications of HCV infection. However, whether HCV itself plays a direct role in the development of HCC and whether all HCV isolates are equally associated with HCC development remain to be determined. HCV core, NS3, and NS5A proteins have been reported to affect a wide variety of potentially oncogenic pathways in cell culture and experimental animal systems.[7] In the present study, we demonstrated that HCV isolates with core-Gln^{70}, NS3-Tyr^{1082}/Gln^{1112} or NS5A-IRRDR≥6 were closely associated with HCC development. In addition, a follow-up study revealed that sequence patterns at position 70 of the core protein and positions 1082 and 1112 of NS3 did not significantly alter during the progression from chronic hepatitis to HCC while NS5A-IRRDR showed a significantly higher degree of sequence heterogeneity in post-HCC than in pre-HCC isolates.

Correlation between polymorphisms at positions 70 and 91 of HCV-1b core protein and IFN-based treatment outcome was extensively studied, especially in a Japanese population.[17-20] Interestingly, the same mutations were also associated with progression to HCC in the Japanese population with HCV-1b infection.[13] Results obtained in the present study confirmed and emphasized the significant association between the mutation at position 70 (core-Gln^{70}), but not at position 91, and HCC development (Tables 2, 3; Fig. 1A). Despite the clinical evidence that strongly supports the correlation between core-Gln^{70} and HCC development, the molecular mechanism underlying this correlation is still obscure. Delhem et al.[36] found that tumor-derived HCV core proteins, but not nontumor-derived ones, interact with and activate double-stranded RNA-dependent protein kinase (protein kinase R or PKR), which might modulate viral persistence and carcinogenesis. Gln^{70} was found in two of the three tumor-derived sequences, whereas Arg^{70} was found in two of the three nontumor-derived ones.

As for the NS3 protein of HCV, the possible link between an N-terminal portion of NS3 encoding viral serine protease (aa 1027 to 1146) and hepatocarcinogenesis was reported.[21,22] However, information about the relationship between NS3 sequence diversity and HCC development is still limited. We previously reported a significant correlation between predicted secondary structure of an N-terminal portion of NS3 and HCC development.[34] In the present study, we demonstrated that HCV patients infected with HCV isolates with NS3-(Tyr^{1082}/Gln^{1112}) were at a higher risk to develop HCC than those infected with HCV isolates with non-Tyr^{1082}/Gln^{1112} (Tables 2, 3; Fig. 2B). Computer-assisted secondary structure analysis of NS3 revealed that Tyr^{1082} was associated with the presence of a turn structure at around position 1083 while Phe^{1082} was associated with the absence of the turn structure.[34] Notably, the catalytic triad of NS3 serine protease consists of His^{1083}, Asp^{1107}, and Ser^{1165}.[37] Since positions 1082 and 1112 are in close vicinity of the catalytic triad, sequences diversity at these positions